



Università
Ca' Foscari
Venezia

Master's Degree Programme – Second Cycle (*D.M. 270/2004*)
in Chemical Sciences for Conservation and Restoration

Final Thesis

—
Ca' Foscari
Dorsoduro 3246
30123 Venezia

Non-invasive Techniques Applied to Cultural Heritage: Raman Spectroscopy and X-ray Fluorescence for the Study of Medieval Manuscripts

Graduand

Carlotta Salvadori

Matriculation Number 834733

Advisor

Prof. Emilio Francesco Orsega

Co-Advisor

Prof. DI. Dr. Manfred Schreiner

Academic Year

2014 / 2015

To my mom...

You use a glass mirror to see your face; you use works of art to see your soul.

George Bernard Shaw

Abstract

This work has been performed at the laboratories of the Institute of Natural Science and Technologies in Arts of the Academy of Fine Arts of Vienna, under the supervision of Prof. Dr. Manfred Schreiner.

Nowadays in the cultural heritage field, non-invasive analyses are more and more widespread, in order to interact as less as possible with the art objects. In fact, the growing demand for instruments directly transportable *in loco*, is followed by the increasing demand of their minimum impact on the materials.

Non-invasive analyses, in fact, not requiring sampling, do not alter the physical and chemical structures of the manufacture, so that the integrity of the analysed artwork is not compromised at all.

The non-invasive techniques chosen in this work were X-ray fluorescence (XRF) and Raman spectroscopy that were applied as complementary techniques in the investigations of medieval fragments made of parchment. These fragments were discovered in 2007, by the *Merowe Dam Archaeological Salvage Campaign*, on the island of Sur in Northern Sudan. This find probably came from a library collection of a church of the Classic Christian Period (11th century). All the fragments and the *folio* were characterised by black and red writings.

In particular, this work aimed to study ancient manuscripts to answer to some questions regarding the inks composition and, if possible, to discover their provenance, as well as for curatorial and conservation purposes. X-ray fluorescence spectrometry and Raman spectroscopy,

in fact, have become one of the optimum tools for the analyses of inks on documents. XRF is very useful to identify inorganic metal-based inks, such as iron gall, vermilion and red lead. Raman spectroscopy, instead, is employed for the investigation of both inorganic and organic inks.

The first part of this work focuses on parchment as writing support with the description of the most inks used. In particular, the development of the parchment among the centuries, its chemical composition, its physical and mechanical properties and the manufacturing steps are described. Moreover, the most applied black and red inks are presented, from both the historical and the chemical point of view. This theoretical part can help to understand the phenomena of degradation of both parchment and inks during the centuries and it is fundamental for the interpretation of the analyses performed on the Nubian find.

The second part of the work, instead, focuses on medieval fragments and *folio*. First, a description of their state of conservation is presented, followed by the presentation and discussion of the results of XRF and Raman experimental analyses performed on inks and parchment.

The experimental results allowed to recognise the nature of the inks as well as the parchment degradation level and the probable different geographical and chronological origins of the fragments and the *folio*.

Table of contents

List of abbreviations.....	xi
Introduction and aim of the project.....	xiii
Chapter 1: Non-invasive investigations in cultural heritage	15
1.1. The importance of non-invasive analyses on artworks	15
1.2. XRF spectrometry	16
1.2.1. Advantages and disadvantages of the technique for artwork analysis.....	16
1.2.2. Nature and properties of X-rays.....	17
1.2.3. Interactions between X-rays and matter	17
1.2.4. Moseley's law	19
1.2.5. XRF instrument.....	20
1.2.6. Qualitative and quantitative analysis	21
1.2.7. Instrument used and experimental conditions	21
1.3. Raman spectroscopy.....	23
1.3.1. Advantages and disadvantages of the technique for artwork analysis.....	23
1.3.2. Interaction between matter and light source	24
1.3.3. The Raman effect.....	25
1.3.4. Origin of Raman spectra	26

1.3.5.	Raman instrument.....	27
1.3.6	Instrument used and experimental conditions	28
1.4.	XRF and Raman spectroscopy applied to medieval manuscripts on parchments...	29
Chapter 2: Parchment as writing support.....		31
2.1.	Parchment historical background.....	31
2.2.	The raw material: animal skin.....	32
2.2.1.	Biological functions and general structure	32
2.2.2.	Collagen: structure and chemical composition.....	33
2.2.3.	Physical properties of collagen	34
2.3.	Transformation of the raw material into parchment	35
2.3.1.	Historical background.....	35
2.3.2.	Manufacturing steps of parchment	35
2.4.	Physical and mechanical properties of parchment.....	39
2.4.1.	Inhomogeneity	39
2.4.2.	Hygroscopicity.....	40
Chapter 3: Inks on parchment		43
3.1.	Historical background	43
3.2.	Inks of ancient manuscripts.....	45
3.3.	Black inks.....	46
3.3.1.	Sepia ink	46
3.3.2.	Carbon black ink.....	47
3.3.3.	Iron gall ink.....	48
3.4.	Red inks	51
3.4.1.	Cinnabar / Vermillion	51
3.4.2.	Lead red	51
3.4.3.	Red earth.....	52
Chapter 4: Degradation of parchment.....		53

4.1.	Main causes of parchment degradation and structural damage.....	53
4.2.	Influence of humidity and temperature on parchment	55
4.3.	Influence of UV light and external contaminants on parchment	56
4.4.	Degradation of parchment by inks	57
Chapter 5: XRF and Raman spectroscopy investigations on ancient manuscripts		59
5.1.	An important find in the Anubis region	59
5.1.1.	Description of the conditions of the parchment find	60
5.1.2.	Conservation and reconstruction treatments	60
5.2.	Experimental	62
5.2.1.	Materials	62
5.2.2.	State of conservation.....	64
5.2.3.	Methods.....	66
5.3.	Results and discussion.....	66
5.3.1.	XRF.....	66
5.3.2.	XRF elemental mapping	75
5.3.3.	Raman	79
Chapter 6: Conclusions		91
List of figures		95
List of tables.....		99
Bibliography.....		101
Acknowledgments		107

List of abbreviations

AD: After Death

BC: Before Christ

CCD: Charge Coupled Detector

DHI: Dihydroxyindole

DHICA: Dihydroxyindole-Carboxylic Acid

EDXRF: Energy-Dispersive X-Ray Fluorescence

HHDP: Hexahydroxydiphenic Acid

ISTA: Institute of Natural Sciences and Technology in Art

LED: Light Emitting Diode

NIR: Near Infra-Red

PGG: Pentagalloyl Glucose

R.H.: Relative Humidity

SDD: Silicon Drift Detector

SEM: Scanning Electron Microscope

XRF: X-Ray Fluorescence

Introduction and aim of the project

This work has been performed at the laboratories of the Academy of Fine Arts of Vienna, under the supervision of Prof. Dr. Manfred Schreiner.

The main aim of this work was to fulfil experimental analyses on the inks and the support of medieval manuscripts made of parchment. In particular, six fragments and a *folio*, discovered in 2007, on the island of Sur in Northern Sudan, were the objects of investigations.

For this scope, the non-invasive analytical techniques X-ray fluorescence spectrometry (XRF) and Raman spectroscopy were chosen.

The ability to combine these analytical methods represented a powerful tool, which could be used to identify the degradation level of the support and the ink type of an already corroded item for conservation-restoration purposes. Moreover, the recognition of the inks could be useful for archaeologists and philologists for geographical and chronological determinations.

Chapter 1

Non-invasive investigations in cultural heritage

1.1. The importance of non-invasive analyses on artworks

According to Lahanier *et al.* [1], the analyses applied to the cultural objects should always be non-invasive, fast, sensitive and multi-elemental. Non-invasive analysis allows keeping the physical and the chemical integrity of the materials in order to avoid the sampling. Fast analysis permits to investigate in short acquisition time a large number of similar objects or performing the measurements on various positions on a single object. Finally, sensitivity and multi-elemental analyses allow not only to study the mayor elements but also to detect trace elements. Both, XRF and Raman spectroscopy fulfil these important requirements.

Nowadays in fact, in the cultural heritage field, non-invasive analysis such as X-ray fluorescence (XRF) and Raman spectroscopy are increasingly widespread and this is due to the necessity to interact least possible with the artworks.

For this purpose, many new instruments were developed over the last few years, being able to perform contactless measurements on the artworks. Most of them are also transportable directly

in loco. Non-invasive analysis allows to study one or more physical-chemical characters, in order to avoid that the object suffers alterations - as would be - instead through sampling.

Especially, for our purposes, XRF and Raman spectroscopy were chosen as complementary techniques for the identification of the materials used in art objects. Since half a century these techniques represent a key analysis for the cultural heritage field. During these last years, in fact, the tools applied to the cultural heritage are finalized not only to the conservation and restoration treatments, but they are also focused on the specific study of artwork, especially about the materials and the technique, in order to gather chronological and geographical information.

1.2. XRF spectrometry

1.2.1. Advantages and disadvantages of the technique for artwork analysis

The X-ray fluorescence (XRF) allows the non-invasive identification of the elements present in the materials used for the manufacturing of an artwork. Usually, it offers the first examination of the artwork without touching it or damaging it in any way [2]. This non-invasive technique presents many advantages such as being useful for the qualitative and semi-quantitative simultaneous analysis of inorganic materials. Furthermore, it can be applied to a big range of elements, and it has a short spectral acquisition time. However, the main disadvantage is that the so called light elements (elements with a low atomic number such as Na, Mg, Al or Si) are difficult to measure in air, limiting the analysis to atomic numbers above 13 (Al), depending on the instrument utilized [3]. Due to the deep penetration depth of the X-ray beam, XRF can not be understood entirely as a surface analysis. Therefore, this analytical method is less applicable for objects with complex stratigraphy because surface texture, heterogeneity and matrix effects can influence the result. Depending on the sample matrix and the characteristics of the instruments, it can be assumed that X-rays can penetrate a few micrometres down to several millimetres causing information overloading of the spectra.

Moreover, XRF does not allow the detection of organic compounds, such as carbon-based materials. Generally, XRF analysis gives information about the elemental compositions of

pigments and inks applied due to the detection of the main elements. Nevertheless, with this technique it is not possible to differentiate pigments of the same class as it provides elemental and not compositional results [2].

1.2.2. Nature and properties of X-rays

X-rays were discovered in 1895 by Wilhelm Conrad Röntgen and are part of the electromagnetic spectrum, in particular between the far ultraviolet and gamma ray region; their wavelength is between 10^{-8} and 10^{-11} m, as it is possible to see in figure 1 [4, 5].

X-rays can be transmitted, reflected, refracted, diffracted, polarized, scattered or photoelectrically absorbed and they can be produced in two different ways: by a deceleration of high-energy electrons (continuous X-rays) or through electronic transitions in the inner orbits of atoms (characteristic X-rays).

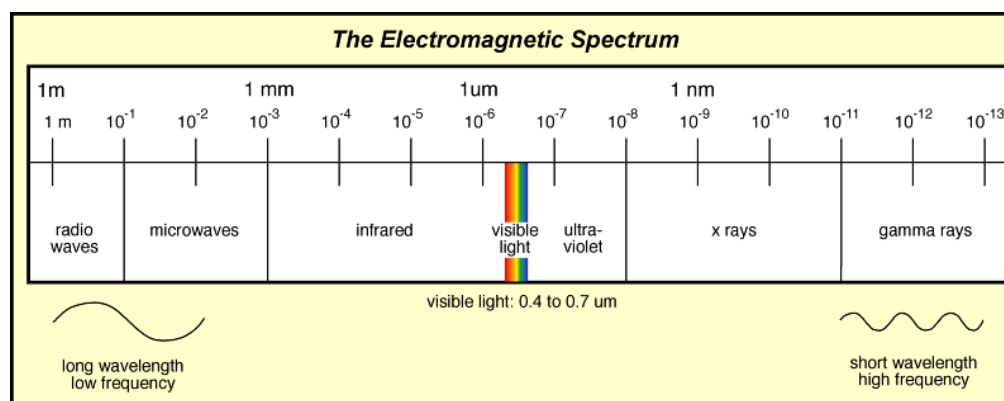


Figure 1. Electromagnetic spectrum [6].

1.2.3. Interactions between X-rays and matter

X-ray fluorescence spectrometry includes the detection and measurement of the energy of the characteristic X-rays produced by inner-shell ionization, which can be used to determine elemental compositions [5]. Each shell of the atoms is characterized by an electron bonding energy that is the minimal request energy to remove an electron from the atom. Especially, when the incident X-ray beam directed on the sample has sufficient energy, it tears the electrons from the inner shells of the atom causing vacancies (this situation is very short and lasts between 10^{-16} and 10^{-9} seconds). This condition confers instability to the atom. The stability is regained when

electrons from outer shells migrate in order to occupy the vacancies of the deeper shells, with the consequent emission of a characteristic X-ray fluorescence [4]. Figure 2a shows this principle. This emission expels a photoelectron (denoted by γ), which energy is described by the energy difference between the excited state (E_f) and the ground state (E_i) of the atom [5]:

$$E_\gamma = E_i - E_f$$

In the characteristic spectra there are specific lines, called K, L, M and N depending on the depth of the shells. It is possible to see in figure 2b the inner shell of the K one, followed by the L, M and N ones.

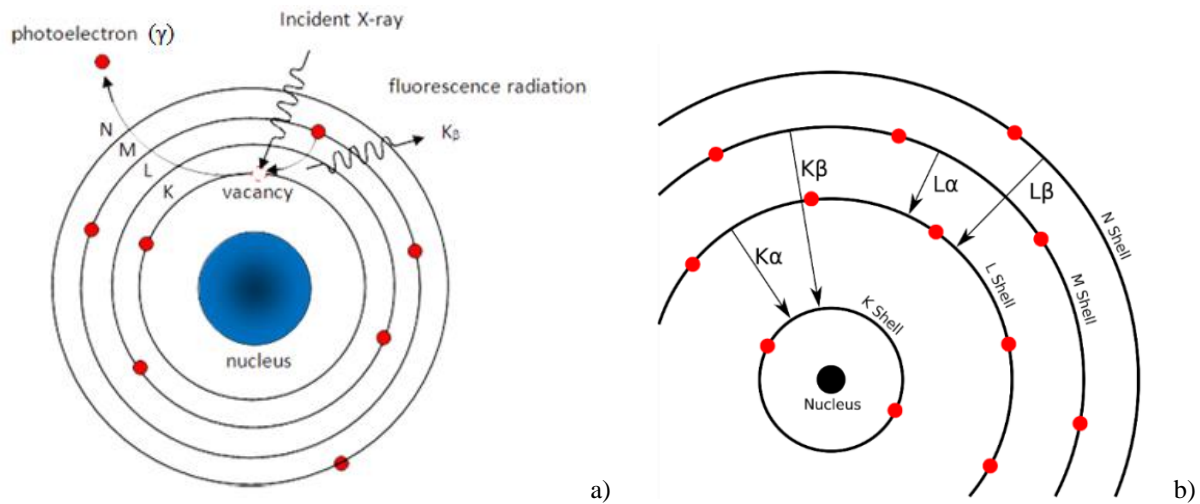


Figure 2. X-ray fluorescence radiation (a) and atomic shells where the electron transitions occur (b) [7].

According to Siegbahn notation, K- and L-lines are divided in K_α (transition from L-shell in order to fill K-shell vacancy), K_β (transitions from M to K), L_α (transitions from M to L) and L_β (transitions from N to L). These characteristic lines are typical for each atom as they are bounded to the atomic number. Both, α and β lines appear always together in the spectrum with defined and constant intensity ratios. In figure 3 an XRF spectrum of a red ink in comparison with the spectrum of the parchment support is shown, in which the characteristic lines of the existing elements can be seen.

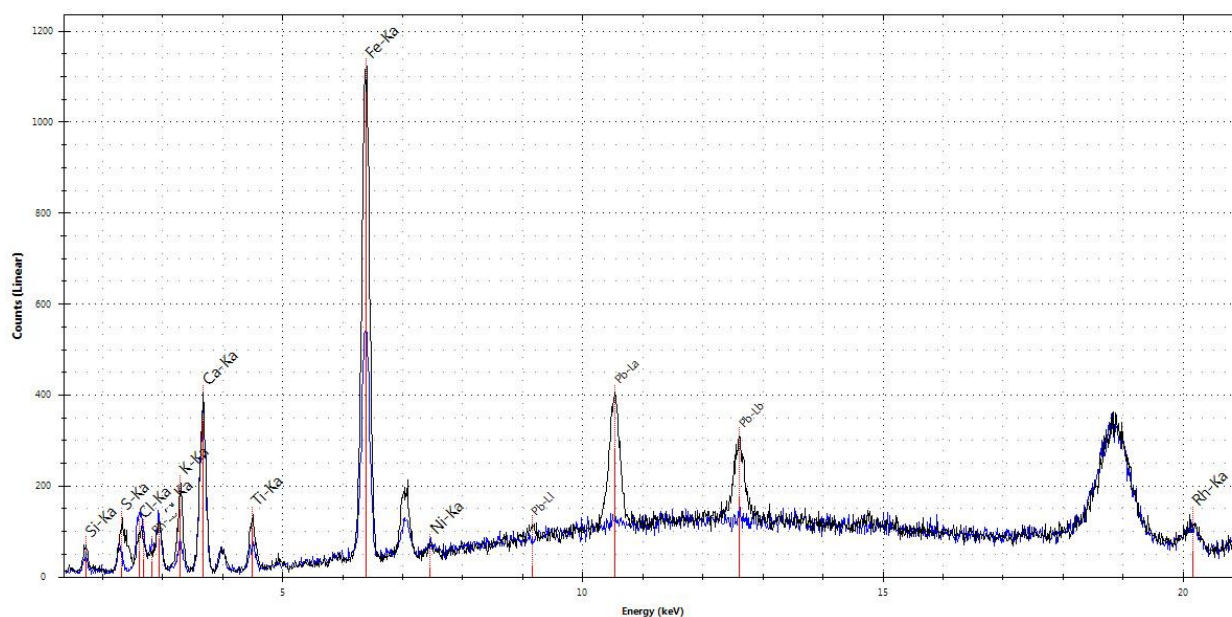


Figure 3. XRF spectrum of a red ink (black spectrum) in comparison with the parchment support (blue spectrum). The typical K- and L-lines of the existing elements can be seen. The red ink is characterised by the presence of Fe and Pb, whereas the elements visible in the parchment are Ca, Si, Cl and K.

It is also necessary to define the fluorescence yield (ω), that is the number of photons emitted of a given series, divided by the total amount of vacancies in the level per time unit [8]. ω increases with the increase of the atomic number. For example the fluorescence yield value of the K shell is less than 0.1 at the correspondence of atoms with $Z < 19$ and this represents a limitation on the analysis of the light elements [8, 9].

1.2.4. Moseley's law

In 1913 Henry Moseley discovered that wavelength (energy) of X-rays emitted by an atom depends on its nuclear charge. He concluded that there was a fundamental quantity, which increases by regular steps from one element to the next [4]. Moseley's law describes the relationship between the wavelength of a spectral line and the atomic number for a given type of X-ray:

$$\lambda = \frac{K}{(Z - \sigma)^2}$$

where λ is the wavelength, Z is the atomic number and K and σ are constants for a given spectral line. σ is equal to 1 for the K-lines and 7.4 for the more shielded L-lines. Based on the fact that Moseley's law says that the energy of an element's spectral line is a function of its atomic number,

light elements spectral lines occur at lower energies than the corresponding lines for elements with a high atomic number. Moreover, peak energies and transition series determine the qualitative identifications of elements [9].

1.2.5. XRF instrument

The chosen instrument applied for the investigation is an Energy-Dispersive X-Ray Fluorescence Spectrometer (EDXRF) equipped with an imaging system. In the EDXRF, all the elements in the sample are detected. An energy dispersive detector is used to collect the fluorescence radiation emitted from the sample and afterwards separates the different energies of the characteristic radiation from each of the different elements in the sample [10, 11].

The main constituents of the used EDXRF instrument are described in figure 4a.

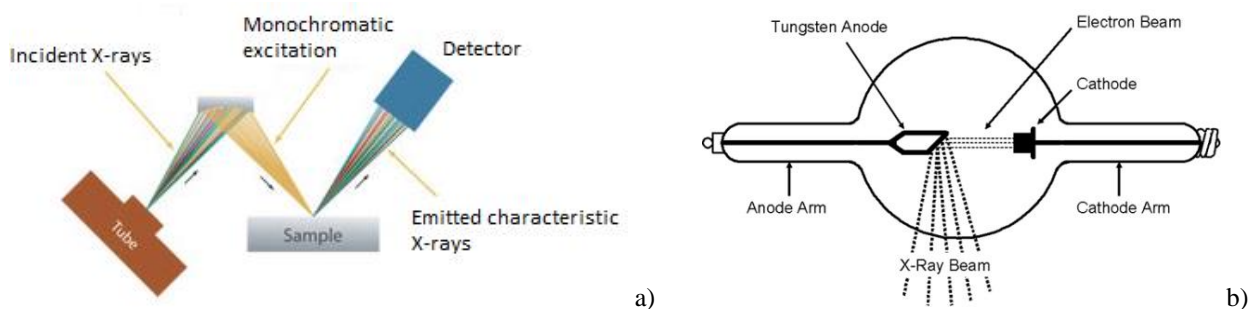


Figure 4. Scheme of an EDXRF instrument (a) [12] and the X-ray tube (b) [13].

The X-ray tube, shown in figure 4b, is a vacuum (glass) tube that produces X-rays. In the tube there are a cathode and an anode. The cathode can be made up of a tungsten filament. This filament is passed through by an intense current that heats the cathode, producing electrons. Due to the application of a potential between anode and cathode, the electrons are accelerated in the direction of the anode, thereby producing an X-ray beam. Finally, a Silicon Drift Detector (SDD), shown in figure 5, analyses the emitted characteristic X-rays from the sample [10]. In particular, the Silicon Drift Detector is based on a high-resistivity silicon material, in which electrons formed by the absorption of ionizing radiation are streamed towards a small collecting anode [10]. In comparison to the usual photo diodes and Si(Li) detectors the SDD detector has a small value of the anode capacitance, which allows to obtain higher energy resolution at shorter times [11]. The detector is integrated with a front-end transistor (FET), which is connected through a short metal strip to the collecting anode. Additionally, the single stage Peltier element installed in the SDD

detector allows to operate with $\text{FWHM} < 145 \text{ eV}$ energy resolution at moderate cooling conditions by avoiding expensive and inconvenient liquid nitrogen cooling in comparison of a Si(Li) detector [11].

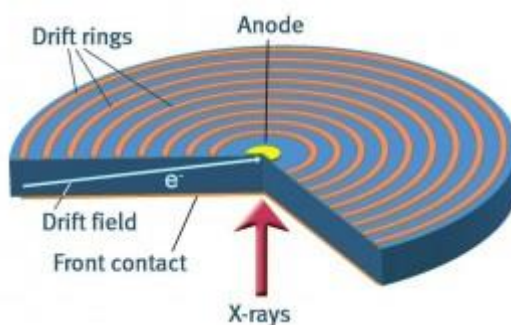


Figure 5. Schematic representation of the Silicon Drift Detector (SDD) [14].

1.2.6. Qualitative and quantitative analysis

Qualitative analysis consists on the identification of the elements present in the sample by measuring the energy of the characteristic X-rays [4]. Nowadays, advanced software are applied for the qualitative analysis in order to simplify the recognition of the peaks and avoid the main interference such as escape and sum peaks. Escape peaks are artefacts occurring when some of the energy carried into the detector by the X-ray photons is absorbed by it, causing the emission of characteristic X-rays. Sum peaks are artefacts that occur when two X-ray photons arrive at the detector simultaneously.

Quantitative analysis is the measurement of the relative amount of each element present in the sample. Unfortunately, not all the artworks can be analysed quantitatively with XRF. Objects with complex stratigraphy are not suitable for quantitative analysis as the heterogeneity of the sample, the surface texture and the matrix effect can influence the result [9, 10]. Mainly semi-quantitative approach can be performed on plain objects such as metals, parchment and paper which are homogenous and do not present many layers.

1.2.7 Instrument used and experimental conditions

XRF analyses were carried out using the ELIO analyser (XGLab, Milano, Italy) shown in figure 6 and the results were elaborated using the Elio Software 1.5.7.7. ELIO is a fully integrated

and portable X-ray fluorescence spectrometer, equipped with an X-ray generator of 50 kV maximum voltage and of 4 W maximum power. It has an Ultra-fast Silicon Drift Detector technology (SDD), covered with a thin Beryllium window and it has two pointing lasers of 690 nm and 1 mm of beam diameter. The objects were analysed with the following parameters: 40 kV of maximum voltage, 20 μ A of tube current and 100 seconds of measurement time. No need for preparation of the object was required. The analyses were done in air and for this reason always the peak of Argon K_{α} was visible. Moreover, the ELIO head can be easily mounted on a light tripod and equipped with translator stages for automatic 1D or 2D elemental mapping with a proprietary automatic scan and analysis software. Two motors mounted with x-y configuration are provided with typical travel lengths of 100 mm.



Figure 6. Portable XRF fluorescence spectrometer instrument, ELIO of XGLab, Milano, Italy.

With the XRF it is possible to perform spot analysis, but sometimes it is difficult to interpret the information of different spots to get an idea about the structure of the whole area. In this case, it is reasonable to use the XRF elemental mapping. XRF mapping, in fact, is a useful tool to gather information about the elements present in the material and it is optimum for applications dealing with heterogeneity in samples. In particular, the elemental mapping capability is excellent for all applications dealing with heterogeneity or concentration gradients in samples and also when impurities or inclusions are found in given specimens. To obtain an XRF mapping, the selected area of interest is scanned in x and y directions with the X-ray beam (figure 7). The corresponding fluorescence intensity is recorded at each point where the beam strikes the object [8]. Moreover, spectral-mapping software allows the user to collect a full XRF spectrum at each point on the mapped area.

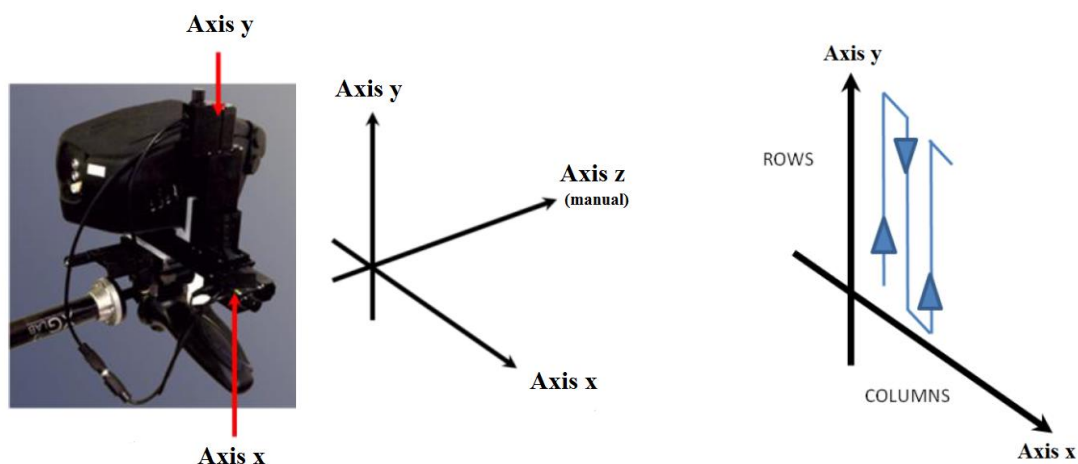


Figure 7. Scheme of the XRF instrument ELIO (XGLab, Milan, Italy) used for the elemental mapping.

1.3. Raman spectroscopy

1.3.1. Advantages and disadvantages of the technique for artwork analysis

In the last few years, the use of Raman spectroscopy for material analysis in art has expanded rapidly [15]. The development of laser sources, detection systems, electronic components, acquisition time, and the important possibility to have portable instruments have increased the use and the quality of Raman analysis. For all these important characteristics, Raman spectroscopy, combining the required attributes of non-invasiveness, reliability and sensitivity, has been applied successfully to the *in situ* analysis and is now recognized as one of the best ways to identify pigments non-invasively [9].

Raman spectroscopy, in fact, is a non-invasive analytical method, where no sampling is required. It can be applied to liquid compounds as well as solid materials and water is not a source of interference. The main advantage is the possibility to distinguish between pigments of the same colour and same composition by detecting the compound-specific molecular vibrations, characteristic for each chemical structure. This technique allows investigating precise functional groups in the molecules for both, organic and inorganic compounds [15, 16].

Main disadvantage of Raman spectroscopy is the fluorescence emission that renders the acquisition of the Raman spectra very difficult. Especially in the case of organic compounds (such as glues and binding media) fluorescence is often masking the Raman features. Fluorescence can be avoided or improved by selecting the most suitable laser source for the measurement. Nevertheless, with the development of new and efficient instruments and softwares, fluorescence problem can be solved with automatic corrections [16]. Possible thermal degradation due to the laser source can occur; therefore, it is recommended to keep the minimum instrumental power/time exposure set-up. An additional drawback of this technique is interferences due to external light. Therefore, measurements have to be performed in dark environments.

1.3.2. Interaction between matter and light source

When light photons interact with matter they can be absorbed, scattered or not interact, passing through it [15]. Absorption takes place if the energy of the incident photon corresponds to the energy gap between the ground state of a molecule and an excited state. This kind of elastic transitions, called also Rayleigh scatter is characterised by no loss of energy. As shown in figure 8, Rayleigh scattering consists on the photon transition from state m to state n [15]. This transition is characterized by an exact energy difference between the two states and it is the most intense process since most photons scatter this way (depicted in figure 9) [17]. Scattering, instead, takes place when a photon interacts with the molecule and scatters from it. An inelastic transition is involved, characterized by a loss of energy (figure 8). In this case there is no need for the photon to have energy which matches the difference between two energy levels of the molecules. Raman spectroscopy uses the scattering phenomenon for molecular identification [15].

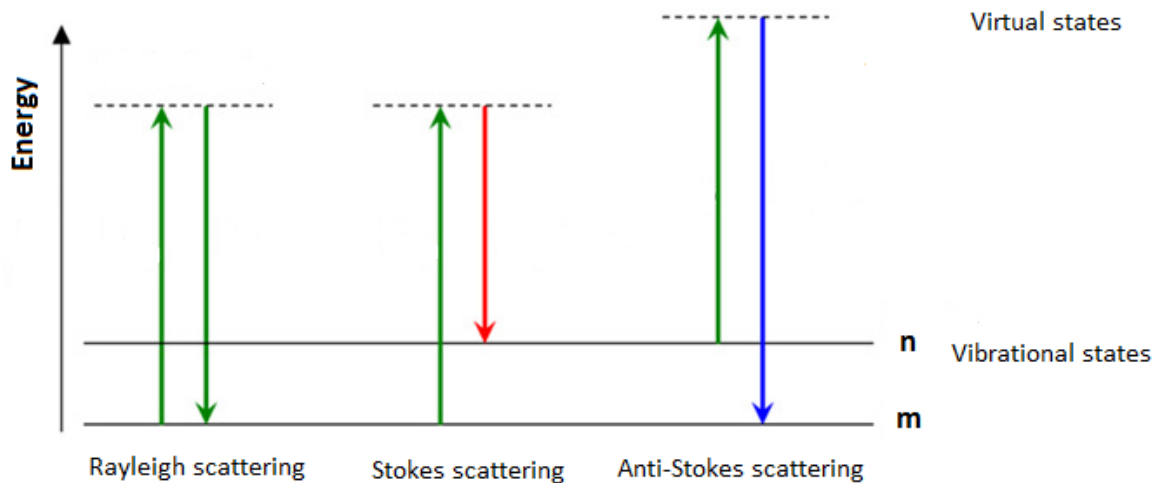


Figure 8. Rayleigh and Raman scattering processes [16].

1.3.3. The Raman effect

Raman spectroscopy is based on the inelastic scattering effect, phenomenon observed for the first time experimentally in 1928 by Raman and Krishnan [16]. Nowadays, in Raman spectroscopy a laser light source interacts with the molecule of the sample and polarizes the cloud of electrons round the nuclei to form a short-live virtual state. This virtual state is not stable and the photon is quickly re-radiated. In contrast to the Rayleigh scattering, Raman scattering measures the difference in energy between n and m states by subtracting the energy of the scattered photon from that of the incident beam. There are two different kinds of Raman scattering, Stokes and anti-Stokes. For both cases the absorbed energy starts from the vibrational state m and ends to the virtual state. The difference between the two scatterings lies in the emitted energy. In the case of the Stokes scattering, the emitted energy goes from the virtual state to the n vibrational state (shown in figure 8.), whereas the anti-Stokes scattering, goes from n state to the ground state m [16].

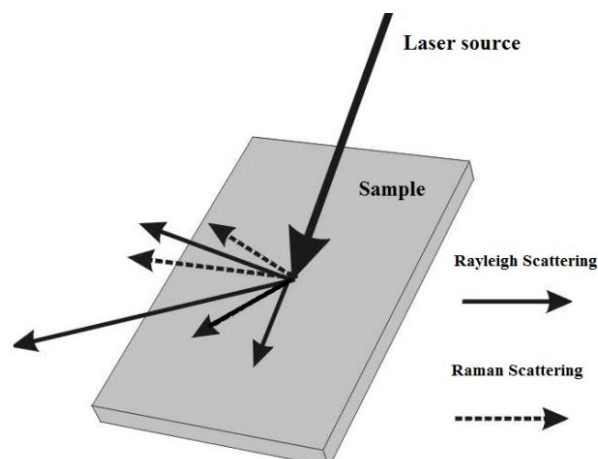


Figure 9. Simplified schematic comparison of Rayleigh and Raman scattering [17].

These scatterings are very rare phenomena, only one photon in every 10^6 to 10^8 photons is subject to scattering. The relative intensities of the two processes depend on the population of the various states. The ratio of the intensities of the Stokes and anti-Stokes scattering is described by the Boltzmann equation [16]:

$$\frac{N_n}{N_m} = \frac{g_n}{g_m} \exp \left[\frac{-(E_n - E_m)}{kT} \right]$$

where N_n is the number of molecules in the excited vibrational energy level (n), N_m is the number of molecules in the ground vibrational energy level (m), g is the degeneracy of the levels n and m , $E_n - E_m$ is the difference in energy between the vibrational energy levels, and k is the Boltzmann's constant of $1.3807 \times 10^{-23} \text{ JK}^{-1}$.

Generally, the majority of Raman scattering is due to Stokes scattering, since these effects have a higher intensity and involve transitions from the lower to upper energy vibrational levels.

1.3.4. Origin of Raman spectra

Each molecule has specific vibration energies. Thus, the vibration spectra are considered as fingerprints of the molecules. The polarizability depends on how tightly the electrons are bound to the nuclei. Raman transitions are related to the polarizability of the molecule, which furthermore depends on the symmetry of the molecular bonds [16, 18]. These vibrations produce typical peaks in the spectra and the observation of a particular group frequency is a confident indicator for the presence of the corresponding structural group in the sample. Triatomic molecules, such as H_2O

and CO₂, have three modes of vibration (γ): symmetrical stretch, bending or deformation mode and an asymmetrical stretch, as shown in figure 10 [15].

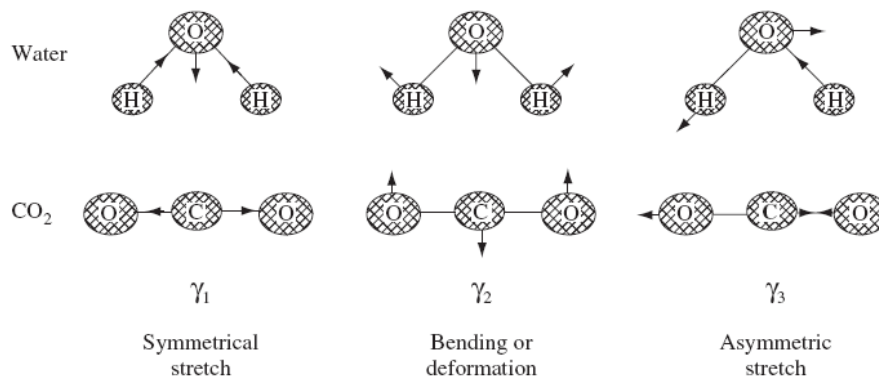


Figure 10. Scheme of the three modes of vibrations for H₂O and CO₂ [16].

Generally, non-polar molecules or groups usually give stronger Raman signals. However, molecules with a centre of symmetry are considered Raman inactive. Consequently, carbonyl groups, which are polar, tend to be not visible, whereas, non-polar molecules without a centre of symmetry like C=C or S=S feature strongly the Raman activity [15].

Each individual spectral band is characterized by three main parameters: vibrational shift, intensity and band shape. The shift or position of a peak in the spectrum depends on the vibration modes and on the bond strength, the intensity depends on the molecular polarizability during the vibration and the band shape on the surrounding [15].

1.3.5. Raman instrument

The Raman instrument chosen for our investigations is a micro-Raman spectrometer which typically consists of four major components: the laser source, a sample illumination system with light collection optics, a wavelength selector (spectrograph) and a detector, shown in figure 11 [15-18].

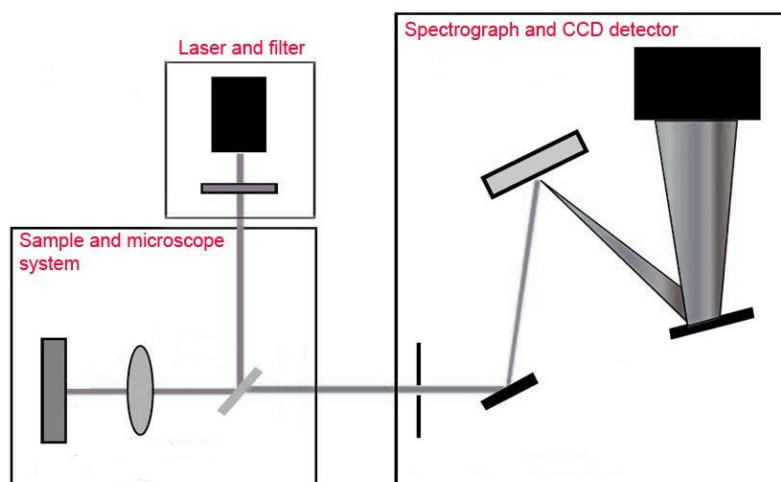


Figure 11. Schematic diagram of the optical path of the Raman system.

The object is placed under a confocal microscope and irradiated by a laser beam (common laser sources are 785, 633 or 532 nm). The scattered light is collected with a lens system, sent through an interference spectrograph and subsequently conveyed to the Charge Coupled Device detector (CCD). The CCD detector is a silicon based multichannel array detector. Its main advantage is the extremely sensitivity to light and allowance to detect the entire Raman spectrum in a single acquisition. CCDs require some degree of cooling (generally $-60\text{ }^{\circ}\text{C}$) to make them suitable for high grade spectroscopy.

1.3.6 Instrument used and experimental conditions

Raman measurements were performed in a dark room using the ProRaman-L-Dual-G analyser of Enwave Optronics (California, USA), shown in figure 12. The results were elaborated with Opus 7.0 software. The ProRaman-L-Dual-G is a fully integrated and transportable Raman spectrometer. The excitation source is a Diode Laser at 785 nm ($\sim 350\text{ mW}$) with a narrow line-width of 2.0 cm^{-1} . The fibre optic probe has a standard working distance of 7.5 mm and it is correlated with a Rayleigh filter. The detector is a two dimensional CCD array temperature regulated ($-60\text{ }^{\circ}\text{C}$) detector. The NIR spectral coverage goes from $\sim 100\text{ cm}^{-1}$ to 3300 cm^{-1} . The integrated microscope is equipped with a 1.3 Mpixel camera with In-Line LED illumination. The samples were measured using a Leica 40x microscope objective (spot size $\sim 50\text{ }\mu\text{m}$).



Figure 12. Transportable ProRaman-L-Dual-G Raman spectrometer instrument of Enwave Optronics (California, USA).

1.4. XRF and Raman spectroscopy applied to medieval manuscripts on parchments

For our purpose, XRF and Raman spectroscopy were used as complementary techniques to analyse pigments and inks on medieval manuscripts made of parchment. X-ray fluorescence spectrometry and Raman spectroscopy have become one of the most important tools for the analyses of both, ancient and modern pigments and inks on documents [15]. Especially, in the inks-field analysis, XRF is very useful to identify inorganic metal-based inks, such as iron gall, vermilion and red lead. Literature reports a lot of case studies in which XRF analysis was indispensable to identify the ink used on ancient parchments and papers [19-23].

Raman spectroscopy, on the other side, is very useful for the investigation of both, inorganic and organic pigments and inks, such as iron gall, vermilion and carbon black inks. For example, Morsy *et al.* [24] were able to discriminate blue and black modern inks. Andermann [25] analysed modern blue and black ballpoint pen inks on paper using four excitation wavelengths (514, 633, 685 and 785 nm) and observed that the quality of the spectrum depends on the chosen laser. Lee *et al.* [26, 27] focused the studies mainly on Middle Ages manuscripts suggesting for the analysis of iron gall inks the use of the 785 nm laser. Further studies performed by Fabianska

and Kuniki [28], focused on the Raman investigation of degradation of blue and black inks for storage and curatorial purposes.

The application of both, XRF and Raman spectroscopy for degradation studies of the parchment support did not show very satisfying results so far. Especially in the case of Raman spectroscopy, due to difficulties in the interpretation of the shifting of the main amide bands in the spectra, it was not possible to define in a certain way the degradation pathway. Raman spectroscopy applied on this field is still under investigation [29].

Chapter 2

Parchment as writing support

2.1. Parchment historical background

Parchment was the most used writing material from the 2nd century BC to the end of the Middle Ages before the introduction of paper. Made of the skin of animals, usually goat or sheep (the finest quality was made of kid skin), after the 3rd century AD it superseded papyrus scrolls for its advantages: durability, stability and economic convenience, while papyrus was a very brittle material, sensitive to humid climate variation and produced exclusively in Egypt [30]. In particular, the opacity of parchment allowed to write on both sides (*rectus* and *versus*) and its solidity was exploited for scrapes, incisions and re-enrols: in the Middle Ages these practices were very common in order to recycle old classical manuscripts and write on them new texts, called palimpsest [31]. The use of parchment dates back 2000 years BC: it was used by Egyptians, Jews, Assyrians and Persians to make musical instruments and writing media. However, there is no certain information about the use of this support in Greece. Mayan and Aztec developed a technique to process the deerskin with smoke and dust of lime. The use of parchment was widespread also in the Roman age, and in *Naturalis Historia XIII, 11*, Pliny the Elder explains that its processing technique was invented for the first time in the city of *Pergamum*. The first books made of parchment took the form of rolls (*volumina*), to recall the shape of papyrus scrolls; in spite

of its elasticity, parchment as a writing support was not entirely appropriate because it did not remain perfectly flat, and it produced a lot of problems to the writer. Between the 1st and 2nd centuries AD, these drawbacks lead to the replacement of *volumen* by *codex* (book), which survived entirely from the 5th century AD. After the introduction of paper in Europe in the 12th century, a long decadence began for parchment, which culminated with the invention of printing, in the 15th century. Consequently, parchment lost its importance as writing medium but its prestige continued for centuries, in particular as a support for official documents, namely for political and administrative ones that needed to be preserved for long periods [32].

2.2. The raw material: animal skin

2.2.1. Biological functions and general structure

Parchment is the result of a complex series of chemical and mechanical procedures, directed towards the transformations of some of the properties of the raw material, i.e. animal skin. Skin is a very complex material, a biological tissue equipped with important precise biological functions: the main ones consist in erecting a defence barrier against the attack of harmful substances and bacteria, receiving an important stimulus from the outside and participating to the water balance of the body [32, 33]. It is a unique material due to its elasticity and reactivity to hydrothermal stimulus and it can tolerate extreme conditions. Its capacity enables to reveal characteristics such as age, sex, diet, stress or state of health of the provenance organism [34]. Skin appears as a strong and very flexible material adaptable to the body anatomic changes. Many of the characteristics listed above play a key role in the degradation study of this membrane because they remain more or less unchanged even after the skin has been transformed into parchment [33].

Three main layers characterize the skin: the epidermis, the dermis and the hypodermis. As it is shown in figure 13, the epidermis is the more external section and generally it consists of covering cells, called epithelial cells, which are hardened by the presence of keratin (the protein that waterproofs the skin). These cells are continually replaced by new material, in order to repair the exfoliated or damaged areas [32].

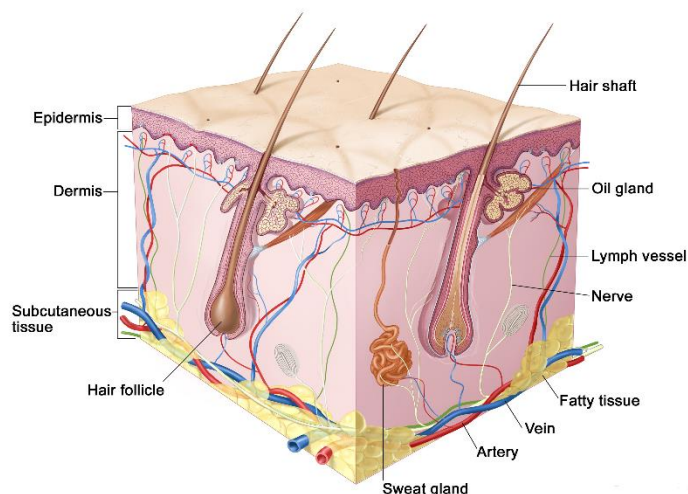


Figure 13. Section of the structure of the skin with the three layers epidermis, derma and hypodermis [35].

Moreover, the hypodermis is characterized by the presence of hair that are originated in the derma. The dermis is the thickest and the most important layer because it is the only one that makes up the most consistent part of parchment. This layer is almost entirely made of collagen fibres that branch out in every direction to form a very strong and resistant network, which is responsible for the extreme solidity and resistance of products made of this material. Besides collagen, in this region there are also reticular and elastic fibres, especially in young skin, that increase the flexibility of the whole web [33]. The derma is divided into two sub-layers: the external one, called papillary, and the internal one, called reticular, that will originate the two opposite sides of the parchment, the grain and the flash side, respectively. Finally, the last and deepest layer is the hypodermis, or subcutaneous tissue, made up of connective tissues, rich in adipocytes and poor in collagen fibres [32].

2.2.2. Collagen: structure and chemical composition

The main constituent of derma is collagen I, the main protein of the animal connective tissue. From the chemical point of view it is a triple helix protein (each chain is made up of about 1000 amino acid residues), called also tropocollagen, stabilized by inter-chain hydrogen bonds and by structural water molecules. The triple helix is about 300 nm long and has a diameter ranging from 1.2 to 1.5 nm depending on its hydration level. The main amino acids in its structure are glycine (about 35% of the amino acidic total amount), proline, hydroxyproline (both about 30%) and, in less quantity, tyrosine and phenylalanine [36]. Especially, this triple helix results from a right-handed coiling around the common axis of three chains, which are formed of repeating Gly-

X-Y sequences, where X is often proline or hydroxyproline. The collagen fibres are randomly orientated and distributed as a felt work [37]. The union of tropocollagens in a longitudinal and parallel way produces fibrils, which are joining with each other and give rise fibres (figure 14).

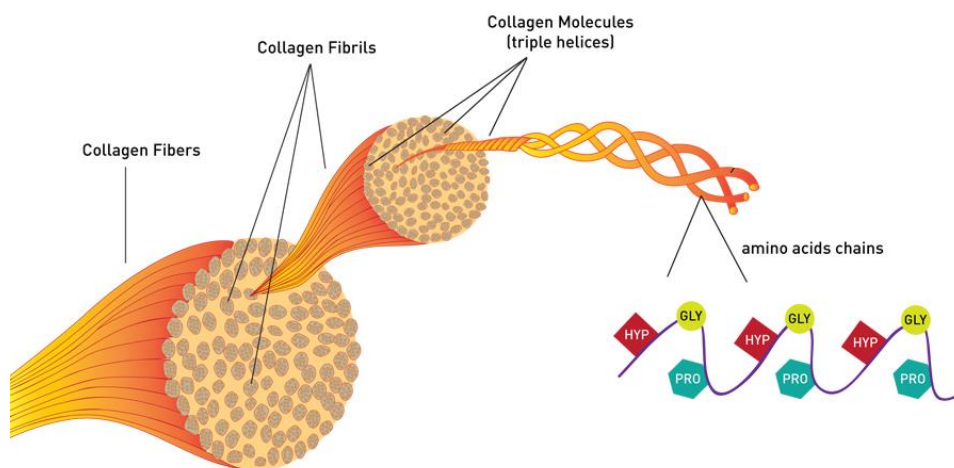


Figure 14. The hierarchical structure of collagen: from the amino acids chains to the fibres [38].

The hierarchical composition of the collagen can be analysed on three different levels: microscopic level, consisting of collagen fibres with a diameter of 0.001-0.1 mm, mesoscopic level, originated by collagen fibril with a diameter of 0.05-0.1 and the deeper nanoscopic level with its micro fibrils of 6-7.5 nm of diameter [37, 39]. Collagen fibres are linked by weak hydrogen bonds, whereas covalent links between terminal ends of the triple helix, carbonyl-water hydrogen bonds, Van der Waals interactions and electrostatic forces hold the collagen hierarchical structure together [32, 40]. The great stability and strength conferred to collagen by this supramolecular structure account for its functional efficiency in a variety of tissues and explain the excellent resistance of documents and artefacts made of parchment [41].

2.2.3. Physical properties of collagen

Collagen and elastic fibres, as elementary units of the skin, give important mechanical properties to the skin. The skin resistant depends on the quantity and density of the collagen fibres, whereas the elasticity depends on their quantity, concentration and the dislocation [32]. Collagen helps to keep the skin flexible and - at the same time - limits any excessive stretching. Moreover - in the adult individuals - the number of epithelial cells gradually increases and the intercellular substance increases exponentially; so, in the upper layer of the dermis the elastic fibres decrease,

progressively stiffening the collagen fibres, while in the deepest layer they swell until they undergo actual lacerations. It is for this reason that young skins were absolutely preferred to the old ones [33].

2.3. Transformation of the raw material into parchment

2.3.1. Historical background

Different from paper, no industrial process of parchment production has ever been sketched out: in fact still nowadays this product is only manufactured and every specimen is unique [41]. The first affirmation of an actual method of manufacturing took place between the 1st and the 2nd century AD when *codex* began to replace the more ancient *volume* definitively. The oldest references - describing the parchment working phases - come from important texts, such as “*Compositiones ad tingenda musiva*” known also as *Lucca manuscript* (Codex 490 of Biblioteca Capitolare di Lucca) and *Schedula diversarium artium*. In the former there is a very interesting recipe, unfortunately short, that describes the main manufacturing steps of parchment; the latter, attributed to the monk Theophilus and dated around 1100 AD, mentions a collection of clear and detailed recipes that have been used by parchment makers for centuries. There was a very long apprenticeship to become an able and skilful parchment maker: this can be testified e.g. in the *Statute of parchment makers of Paris* of 1545-1550, drawn up during the reign of Francis I. and Frederick II. and later amplified by Louis XIV. in 1654, in which the indispensable conditions (e.g. at least seven years of experience) for receiving the title of “Master Maker of Parchments” are described [33].

2.3.2. Manufacturing steps of parchment

The manufacturing of parchment followed different procedures depending on the geographical area and historical period. The commonly intended meaning of the word “parchment” is related to the western method carried out since the Middle Ages. The manufacture of parchment was a procedure based on depilation, soaking on lime, drying under pressure and

stretching by scraping the skin. Especially the unchanged manufacturing of parchment took place through the following steps [32, 33]:

1. *Choice of the raw material*: The skin had to be of good quality in order to guarantee the success of the final product. Parchment, in the first instance, was obtained from the working only of sheep skin and it was only at a later date that the skins of calves were also used [32]. The most prized and expensive type of parchment was the “*vellum*”, the skin of the young animals, famous for its lightness, smoothness and transparency [42]. It was important that animals were in good health conditions and, especially, without any skin disease.
2. *Flaying*: It consisted on the separation of the skin from the dead animal.
3. *Conservation*: As the skin was not always suddenly used, it was subjected to salting in order to avoid the putrefaction. This step could be made in dry or in wet conditions: The first method consisted in the scattering of sodium chloride or potassium chloride on the skins, whereas the second one consisted in the immersion of the skins in saturated solutions of NaCl for 3-4 days. Both treatments were useful to reduce the amount of water in order to better preserve the skins [33].
4. *Reviving*: It was a re-hydration process during which the skins were dipped in cold water. This step was useful also to remove salts, dirt and the soluble substances [32].
5. *Soaking in lime*: During this very important step, skins were dipped in saturated solution of calcium hydroxide, $\text{Ca}(\text{OH})_2$, in order to remove the hair. This phase, that lasted minimum 8 days (for thinnest skins) and maximum 30 days (for the thickest ones), allowed to weaken the epidermis, to swell collagen fibres and saponify the fatty component, making it soluble (Figure 15) [32].

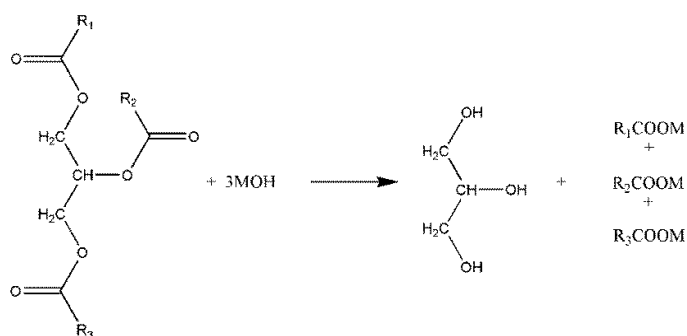


Figure 15. Saponification reaction: triglycerides contained in the animal skin react with $\text{Ca}(\text{OH})_2$ in order to produce free fatty acids.

Especially, the major chemical modification of collagen during this step was the hydrolysis of some of the amino groups attached to aspartic and glutamic acid residues [43].

Sometimes sodium sulfide, Na_2S , was used in addition to $\text{Ca}(\text{OH})_2$ to decrease the time of the soaking in lime. Na_2S solubilizes keratin, the protein of hair and epidermis, and facilitated the depilation step. In particular, Na_2S with the presence of calcium hydroxide reduces the amino acid cistin into two molecules of cysteine, through the break of disulfide bridge (S-S), making keratins soluble (figure 16) [32].

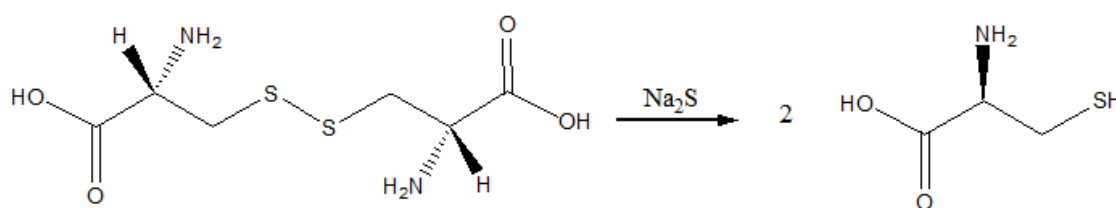
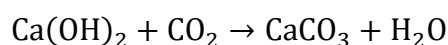


Figure 16. Amino acid cistin is divided into two molecules of cysteine, through the break of disulfide bridge due to the presence of Na_2S .

6. *Depilation:* Through this operation, the hair was manually removed with a special not sharpened knife or a smooth stick in order to preserve the derma layer. Usually this step took place during the springtime because parchment worked in winter was always of poor quality: especially, frost produced a shrinking of the skin so that the roots of the hair became much more tenacious and more difficult to remove [42].
7. *First washing:* Skins were left in water for 3-4 days to remove the excess of $\text{Ca}(\text{OH})_2$ and the soluble products. A certain amount of calcium hydroxide remained always in the parchment and in contact with the air it was transformed in calcium carbonate, CaCO_3 , according to the following reaction of carbonisation [32]:



Calcium carbonate conferred to parchment an alkaline reserve, making the skin whiter and more opaque.

8. *Assembling on the loom:* Skins were spread on wooden looms; young skins were prepared winding some areas to little stones that were fixed with a robust string and then assembled on the loom; the old ones, instead, thicker, were directly fixed on the loom with nails [32].

9. *Scraping*: This step allowed to separate derma from hypodermis with the use of a special crescent shaped knife; dermis layer, or *corium*, was composed of approximately 95% collagen [33].
10. *Second washing*: Always on looms, skins were washed with water.
11. *Drying under tension*: This step was very important because it determined the final characteristics of a sheet of parchment. Skins usually were dried in airy places. When water evaporated, skin suffered contractions and, being bounded to the loom, was submitted by further and gradual traction. This traction forced the fibres to arrange themselves in parallel to the surface. Water evaporation, furthermore, allowed parchment the formation of inter-fibre-bonds that contributed to give to it compactness, force and resistance. Usually, parchment was not exposed to sun, humidity and frost during the drying step, as possible damaging could occur. Sun, in fact, produced an excessive shrinking of the fibres which weakened the skin, making it less strong and easier to tear; humidity (or rain), instead, caused dark stains, probably due to the presence of mould; finally, frost ruined the skin producing a shrinkage [42].
12. *Polishing*: During the drying phase, when parchment wasn't completely dried, the polishing step took place, usually carried out with pumice stone in order to obtain a homogeneous and plain surface [32].
13. *Finishing treatments*: However, at the end of all these processes, the sheet of parchment was not completely ready for use because it was too smooth and greasy and not suitable to receive inks and pigments. Many times several degreasing treatments were used, depending on the geographic areas. Often ox gall (a gentle natural surfactant) and alums (mordant that allowed to obtain a partial tanning) were used. Moreover, often a preparatory layer of gypsum, clay or chalk mixed with arabic gum or fish glue and also egg white or linseed oil was applied to give more brilliance to the surface and also to protect it from humidity. Poorer parchments were treated with chemical preparations such as sodium sulfite (Na_2SO_3) suspended in natural oils; thereby, a more translucent material simulating the finest vellums was created [30]. All these techniques were very common in Bisanzio, during the Eastern Roman Empire. Instead, e.g. for the Jewish tradition the parchment finishing with vegetable tannin and oil was common: of course, tannin was applied in much smaller amounts than the ones needed in leather tanning [44].

-
14. *Cutting process*: At the end of all these steps, parchment was cut into sheets of specific dimensions in order to transform them into a writing support.

2.4. Physical and mechanical properties of parchment

The most important qualities of parchment are permanence and durability [32]. Permanence consists of maintenance of the main properties for a long time, without significant damages in normal conditions of use and conservation. Durability is instead the property of a material to repeatedly resist to mechanical stresses. These two features have always made parchment robust and resistant to the external solicitations and hence, exceptionally long-lasting. Especially, from the physical point of view, this membranaceous material is characterised by inhomogeneity and hygroscopicity.

2.4.1. Inhomogeneity

Inhomogeneity depends on animal features and history (species, age, health, sex etc.) and on the different methods of manufacturing that both determinate the uniqueness of each parchment sheet [32]. Especially, critical phases were the soaking in lime and the drying step under tension: the first one, through different treatment time and the possible addition of Na_2S , could change some characteristics of the final product, such as fibre integrity and rigidity, while, the second one could cause the flatness of the sheet. For example, there are differences in weight, thickness, stiffness and tensile strength not only between different sheets but also into the single one. Some studies show that some physical and mechanical properties, such as weight, thickness, density and rigidity can change in the same sample of parchment [32]. Generally, higher and lesser values of weight and rigidity correspond to the backbone and abdomen area, respectively and also the distribution of values of breaking load are similar to the weight values. Moreover, the Young's module is very different from sample to sample and also its distribution in the same one can be completely random. Many studies demonstrate the impossibility of schematizing the behaviour of parchment and preclude the possibility of using mathematical models to explain different behaviours [45].

2.4.2. Hygroscopicity

Hygroscopicity is closely connected to the capacity of parchment to exchange water vapour with its surroundings [33]. This property is caused by the presence of collagen that, with its several polar groups, is able to bond water molecules from outside through hydrogen bonds. The total amount of water inside parchment depends on the surrounding environment: humidity promotes the formation of intra and inter molecular interactions and allows water absorption, following by an increase of weight, whereas a dry climate tends to transfer water molecules from parchment to the environment with a decrease of weight (figure 17) [32].

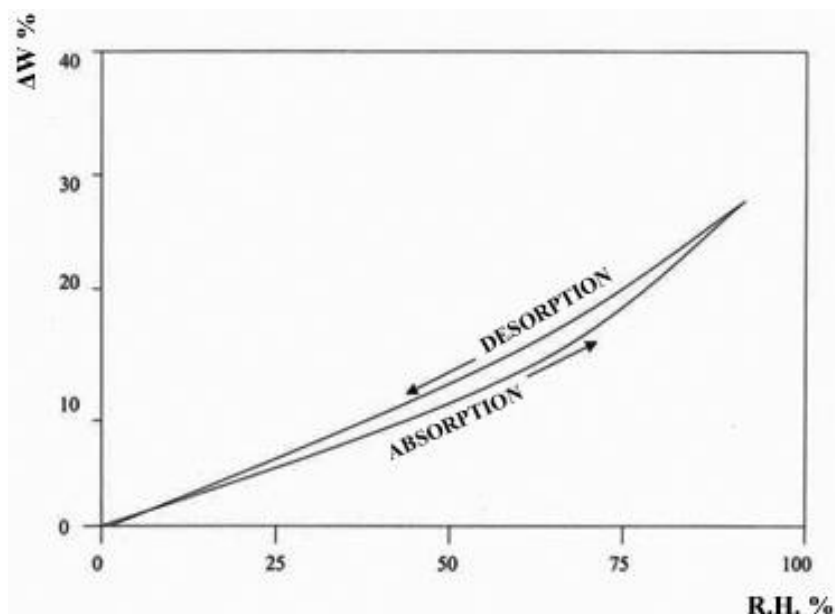


Figure 17. Hygroscopic hysteresis of parchment: the process of absorption is different from the process of desorption: the first curve describes how the humidity of parchment increases when the air relative humidity is carried from zero to 100%, whereas the second one shows the opposite behaviour [32].

Some studies have shown that a sheet of parchment contains about 10-13% of its weight in water at 50% in relative humidity (R.H. %). When the environment R.H. increases up to 70-80%, the water content in the parchment reaches about 25%, while under air saturation conditions, (R.H. about 95%) the total amount of water in parchment reaches 35%. This process happens gradually in a time from two to four days and allows parchment to enter into balance with its surroundings, as presented in figure 18 [32].

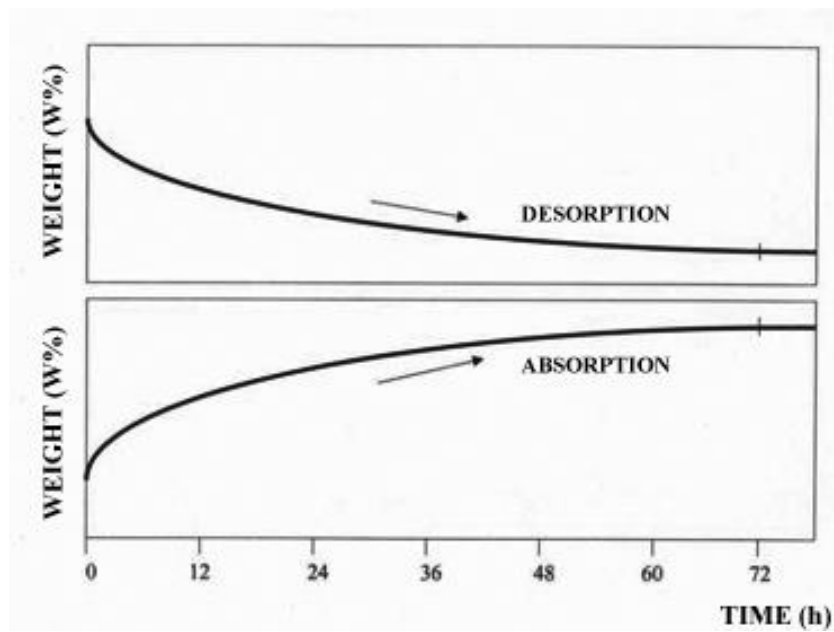


Figure 18. Typical curves of absorption and desorption of parchment: after about 72 hours, the total amount of water becomes constant, and consequently also its weight [32].

If parchment stays long time and/or several times into an environment high humidity, water would be stabilised in it and will cause damages and degradation [32, 34].

Chapter 3

Inks on parchment

3.1. Historical background

The word “ink” comes from the ancient Greek *enkauston*, that means burnt, cooked, probably alluding to carbon black, the main ancient source for black inks, coming from the combustion of various type of wood species or plant waste [46]. Inks, used generally liquid, are characterized by two main constituents: the colouring fraction and the vehicle or binder. The first one is obtained by inorganic pigments or organic dyes, and the second one consists of a fluid that allows to keep pigments in suspension and to transfer them easily on the writing support. Dyes are solubilized by the binder, whereas pigments are dispersed in it and confer own hue and saturation [46].

Probably the first ink was made in China between 2700 and 2600 BC and it could have been invented by T' ien Ciù. This ink seemed to be prepared with a fine powder of a dark stone with a lacquer that gave it a particular brilliance [47]. Nevertheless, the first sure and known recipe, dating on V–IV century BC, is described in the book *Tsi Min Jao Shu* of Kia-se-che, in which it is recommended to mix lamp black with an oil binder (probably tong or sesame oil). Chinese utilized a lot lamp black and carbon black with glue and oil as a binder and, over time, they used to give to inks the shape of solid little sticks that, before the use, were diluted in water. The manufacturing

of inks was so important in the Chinese world that inspectors of the emperor controlled their quality directly [46]. Ancient Egyptians, instead, used to make black inks with soot or charcoal with vegetal oil, arabic gum and glue, whereas for the red hue they utilized red ochre finely dispersed in the same binders. The use of sepia was also very common, in particular to write on stone [32]. Scribes used inks in the shape of cakes or sticks that dissolved in water with the help of a little pestle; the use of both, black and red pigments was widespread and often scribes were represented with one *calamus* in a hand, whereas the second one put in the upper lobe of the ear, as it is shown in figure 19 [46].



Figure 19. Particular of a bas-relief found in Corbis dated 2450 BC in which two scribes writing with two *calami* are sculpted [46].

In the Arabic world, in the same period, a particular ink called *dejo* - a mixture of lampblack, arabic gum and vegetal juices - was hardly used [48]. From Egypt, the manufacturing of ink arrived in Greece and then in Rome, but unluckily there are no direct notices about its use among Greeks. Important Roman testimonies about the use of inks are *De architectura* of Vitruvius (80/70-23 BC), *Naturalis Historia* of Pliny (23-79 AC) and *De materia medica* of Discoride Pedanio (about 40-90 AC). In the first one the ink is described as a mixture of lampblack, obtained by burning pitch and vine wood with arabic gum or fish glue. Pliny, instead, says to make the *atramentum* using the soot obtained by burning resins or pitch. Moreover, both Vitruvius and Pliny describe a furnaces system to burn the wood or the pitch in order to obtain the black pigment. At last Discoride reports an ink made by three parts of lampblack and one part of arabic gum. In any way, all the Roman recipes of black ink contained carbon black (coming from different raw materials) mixed with binders such as animal glue, arabic gum, honey and egg white and then traded in the shape of sticks or sticky tablets. Usually also vinegar, garlic juice or cloves were added to better conserve the mixture [32]. In ancient Rome the red ink was also utilized, usually made of cinnabar or red earth; red hue was very employed for titles and laws. Purpura ink, the most expensive dye, was utilized only for the emperor signature [32, 46, 49]. Pliny moreover,

describes in *Naturalis Historia* the first embryonic manufacture of a particular ink that was known in the Middle Age as iron gall ink: in a ferric salt solution a decoction of gallnuts with peel of pomegranates was added in order to obtain a useful pigment to write. According to the Roman author, sometimes also other substances were added to the black ink, such as *misya*, a yellowish earth, and *salsugo*, a mineral sediment based on copper sulphate with iron impurities. After the 2nd century AC the use of inks became widespread: the discover of ancient recipes allowed the production of ink directly on site and the import of the Chinese ink gave to the decadent Roman Empire high quality manuscripts. After the fall of the Empire inks were of bad quality due to their high costs caused by the lack of commerce: this is the reason why many manuscripts of that period are not nowadays in good conditions. During the Middle Ages, where the writing was entrusted to the monks, three categories of ink were mostly in use: firstly, those made of carbon particles (soot) dispersed in binders like arabic gum or animal glue (very similar to Roman inks); secondly, mixed inks, made of soot and gallic-metal compounds; thirdly those made of phenol acids mixed with iron or copper sulphate (gallic-metal), bound with arabic gum or tragacanth [33, 50]. The replacement of the carbon black ink with the iron gall one from the 3rd century AC was caused by the facility to remove the first one with simple abrasion: it was necessary to utilize a more resistant ink, like the iron gall one. The latter was made up with a mixture of gallic and tannic acids (generally obtained from gallnuts) and iron salts. An important witness about the use of iron gall ink is from the *Schedula diversarum artium* of Teofilus (11th century), in which an ink made of concentrated solution of tannic acid with vitriol (iron sulfate) is described [46]. This kind of ink will be widespread until the 13th century. It is clear that over the time, the formulation of inks became more complex, till nowadays, where the inks are mainly industrial products, in which the raw material is often iron gall ink.

3.2. Inks of ancient manuscripts

The inks mainly used to write on parchment were the black and the red ones. From Egyptian to the Middle Ages the raw materials to obtain both inks were almost the same but mixed in different types of binders. The most used binder was arabic gum, a polysaccharide produced by some species of *acacia*, mostly widespread in Africa. In the next paragraphs, both from the

historical and chemical point of view, the most used black and red inks used on parchment are described.

3.3. Black inks

For the writing of ancient parchment manuscripts, black ink was obtained from a great number of different pigments and dyes, which can be divided in three fundamental kinds: sepia, carbon black and iron gall ink.

3.3.1. Sepia ink

It is one of the most ancient inks and it was obtained from a small gland of the namesake mollusc (*Sepia Officinalis*), widespread in the Mediterranean Sea. Its hue is not properly black, but dark-brown, with a reddish shade and a particular transparent texture. Especially, this organic dye was widespread as ink among Egyptians [51]. The main component is eumelanin (shown in figure 20), the chemical structure of which is still now under investigations.

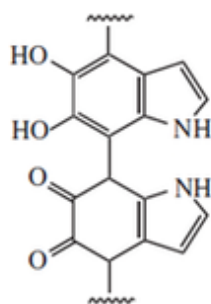


Figure 20. Chemical structure of eumelanin, which it is a complex polymer of 5,6-dihydroxyindole (DHI) and of 5,6-dihydroxyindole-2-carboxylic acid (DHICA) [52].

Sepia is not a reactive ink; it is soluble in alkaline solutions and does not react with other pigments. It can be bleached by nitric acid or other oxidants [52]. It is characterized by a slow drying and for this reason, it was very common to add to it some ashes, which served as absorbent and desiccant [46].

3.3.2. Carbon black ink

It is probably the most commonly used black pigment in the ancient world for writing. Its use was known since 2500 BC and especially documented among Egyptians, Greeks and Romans [53]. It is made up by elementary carbon (88.3–99.5%) with several impurities (such as ash and tarry materials) [32]. There are three main varieties of carbon black: the first one, called specifically black resin, was obtained from the combustion of resinous woods (especially beech wood and cork) or from calcination of resins like rosin. The second one was obtained from the combustion of substances used for lamps or candles, such as pitch, olive, linseed or hemp oil and stearic fatty acids. The last one was obtained by the combustion of branches of vine and also it contained a little quantity of potassium salts [32, 51]. It is very difficult to distinguish among the three forms, also with the help of a microscope. The manufacturing of carbon black took place in particular terracotta containers, in reducing atmosphere: through serpentine passages, the smoke sedimented in the form of black dust, thin and light [51]. Generally, carbon black is a stable and inert pigment, which does not react with other substances, like air pollutants or pigments, but recent studies have demonstrated that during the burning process also retenes (shown in figure 21) and related aromatics, which are not chemically inert can be produced. These molecules absorb ultraviolet light and become chemically active producing free radicals that can attack the polysaccharide bindings and thereby compromise the adhesion of carbon black inks to the substrate surface [54].

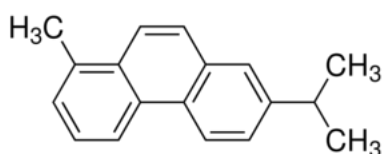


Figure 21. Retene chemical structure. It comes from the burning process of terpenes (saturated hydrocarbons) contained in resinous woods.

Disadvantages of carbon black are that it was not deep penetrating and then it was prone to be easily rubbed off [32]. Moreover, the carbon particles settled out if ink was in a liquid form and had to be regularly stirred to re-suspend the particles [53].

3.3.3. Iron gall ink

Since carbon black ink could be easily removed from the support, starting from the 3rd century BC a small quantity of iron sulfate was sometimes added to it. This salt, in fact, being water soluble, could penetrate in the parchment fibres resisting to the rubbing better [32]. However, it produced brown encrustations, due to its transformation in iron oxides over the time. When the reaction between tannin acid and iron salt was known, this problem could be solved, obtaining a mixture of carbon black and iron gall ink [55]. Probably this is the most accredited hypothesis about the origin of iron gall ink. Especially, this kind of ink was widespread throughout the Middle Ages.

The main ingredients of the iron gall ink are tannin, vitriol (source of iron sulfate) and usually arabic gum as binder. The most used solvent to mix these ingredients was water and often white wine, which increased the solubility of tannic acid and preserved parchment from biological attacks [32].

Tannins, from the chemical point of view, are high molecular weight polyphenols and are divided in hydrolysable and condensed tannins. The first ones, the most interesting for this purpose, can be also divided in gallotannins and ellagitannins. The gallotannins, as can be seen in figure 22, are simple polygalloyl esters of glucose and the prototypical gallotannin is pentagalloyl glucose (PGG) known also as tannic acid [56].

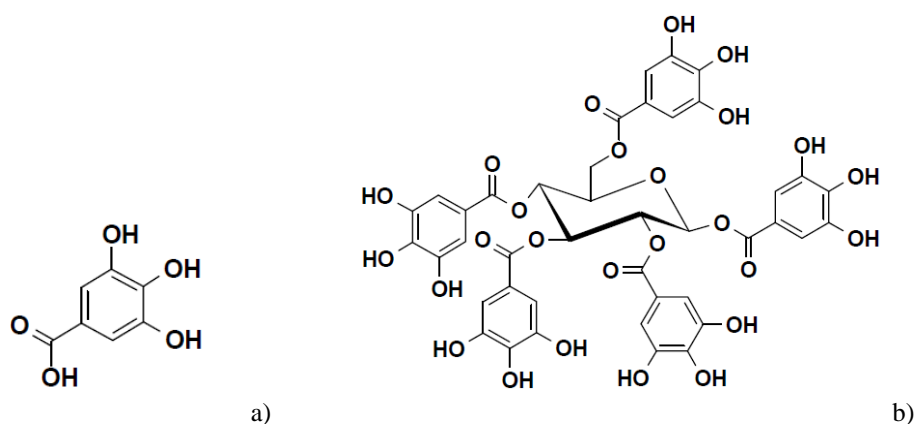


Figure 22. Chemical structures of gallic acid (a) and tannic acid (pentagalloyl glucose or β -1,2,3,4,6-pentagalloyl-O-D-glucose) (b) [56].

Like all gallotannins, PGG has two isomers, as it is shown in figure 23.

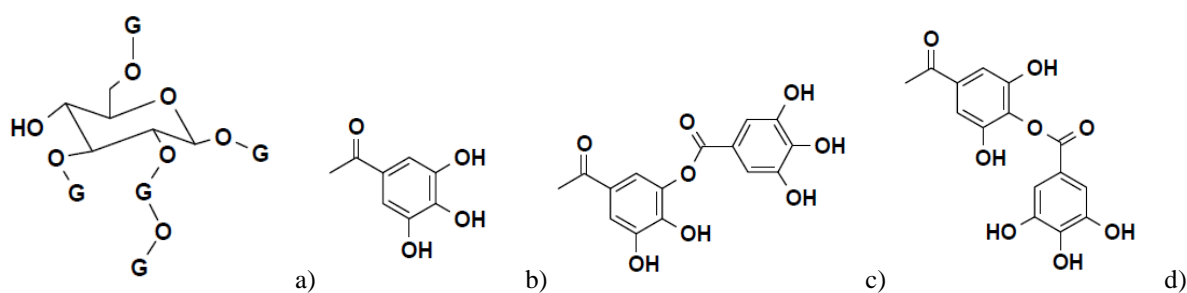


Figure 23. Chemical structure of β -1,2,2,3,6-Pentagalloyl-O-D-Glucose (a), where: G = galloyc ester (b), GOG = digalloyc ester, meta-depside bond (c) and GOG = digalloyl ester, para-depside bond (d). The molecular weights of all the isomers of PGG are the same (940 g/mol), but the chemical properties depend on the different structure [56].

Ellagitannins, instead, are esters of hexahydroxydiphenic acid (HHDP) formed by the oxidative coupling of galloyc groups. HHDP spontaneously lactonize to elagic acid in aqueous solution (figure 24).

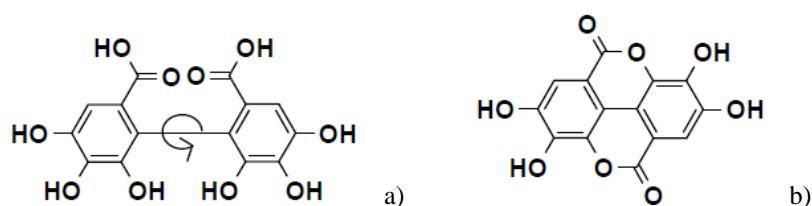


Figure 24. Chemical structure of HHDP (a) formed by the coupling of galloyc groups and converted in elagic acid in aqueous solution (b).

Gallotannins, after hydrolysis, give gallic acid and glucose, whereas allagictannins yield gallic acid with other acids (such as eugeniin and casuarictin), and glucose.

Tannins, and the gallic acid, were usually extracted from the maceration of gallnuts (figure 25), outgrowths of various shapes and size that grew up on some parts of plants after the bite of particular insects [32].

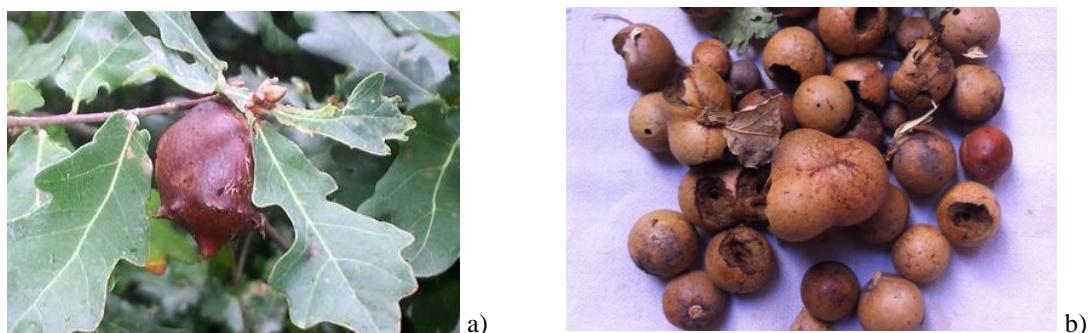


Figure 25. Examples of oak gallnuts, fresh (a) and dried (b).

The formation of ink depends on the reaction between the organic tannins and iron sulfate. Especially, at the beginning, on combination of the iron(II) ions with organic gallic acid, an iron(II) complex is formed, as it is shown in figure 26 [57, 58]. Moreover, the reaction between H^+ and Fe^{2+} causes the formation of sulfuric acid.

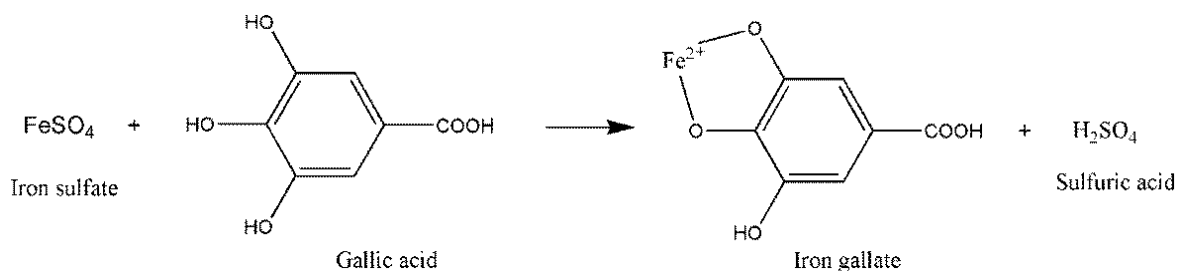


Figure 26. Acid-base reaction between gallic acid and Fe^{2+} ions through which an iron(II) complex is formed [58].

This complex is water soluble and gives a weak grey hue to the ink. Once it has been written on the parchment and exposed to oxygen present in the air, this iron(II) complex easily oxidizes in three-four days and then the resulting compound responsible for the black ink is believed to be iron(III)pyrogallate complex (figure 27).

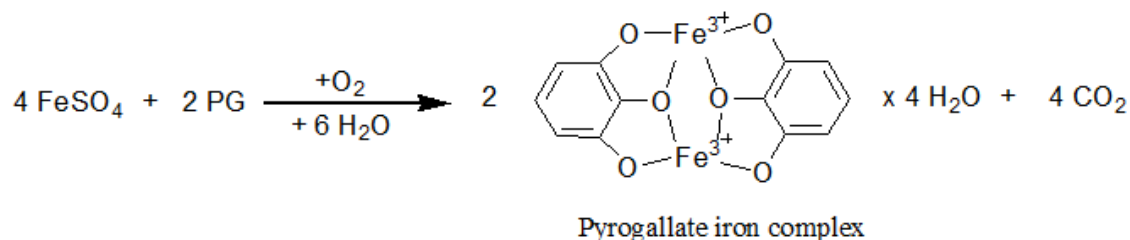


Figure 27. Redox reaction in which four molecules of iron sulfate react with four molecules of gallic acid in order to form two molecules of pyrogallate complex and four molecules of water and CO_2 [58].

This iron(III) complex is black and insoluble in water. The formation of CO_2 , due to the break of the carboxylic groups of the iron pyrogall, layered over the ink, protects it from further oxidation [58].

Since the iron(III)gall ink just prepared had not an intense black colour (in fact few days of oxidation were necessary to obtain the black hue), carbon black or other organic dyes were often added, in order to give a darker hue that allowed his immediate use [55]. The slowness of the oxidation process was a good thing because in this way the iron(II)gall ink, being soluble, could go deep into the parchment, dyeing the collagen fibres. This contact between these two materials gave to the ink a great resistance to UV light, solvents, external agents and especially to possible removal attempts.

Sometimes, to revive illegible writings, a decoction of gallnuts was applied by brush in order to remake directly on the writings the iron(III)complex; but this practice had the tragic consequent to darken irreversibly the treated area [55].

3.4. Red inks

The use of red inks was also very common in ancient manuscripts, particularly to write titles or important texts. Below are listed the three main red pigments used from the ancient world to the Middle Ages.

3.4.1. Cinnabar / Vermillion

This pigment was employed in all the ancient world, since Egyptians, through Greeks and Romans, to the Middle Ages [51]. It was extracted from a bright red mineral and, from the chemical point of view, it is a mercury sulfide (HgS). It was considered a kingly pigment for its intense and evocative hue. Unluckily it is not very stable to sun UV radiations: ancient documents report and describe its tendency to become dark. This hue variation is due to the transformation of the trigonal α -HgS (red) into the polymorphous cubic β -HgS (black) form. It was also common to use the synthetic cinnabar, known as vermillion, already produced in the post-classical period; particularly, its use was widespread during the Middle Ages.

3.4.2. Lead red

It consists on a lead-based red-orange pigment of the chemical formula Pb_2PbO_4 or $PbO \cdot PbO_2$, extracted from the same mineral. Since the first century AD, this pigment was produced in a synthetic way because of its low availability in nature [51]. It was obtained by heating other lead-based compounds, such as lead white and litharge. Especially Vitruvius in *De architectura* underlines the higher quality of the synthetic one compared to the natural one. Lead red is very reactive to sun exposure (loses its original hue) and changes its colour in contact with acidic substances. Nevertheless, it is very stable in oils (often used as ink binders), and this compatibility is due to the possible formation of lead stearates (originated from the saponification reaction

between the fatty acids of the binder and lead metallic ions of the pigment) which led to the formation of crystalline aggregates making the final film stronger and more elastic [51].

3.4.3. Red earth

Called also red ochre, this natural pigment is made of α -hematite, α - Fe_2O_3 and impurities of clays, $\text{Al}_2\text{O}_3\text{SiO}_2 \cdot x\text{H}_2\text{O}$. The percentage of hematite, usually between 63-97% causes the final red hue [51]. Especially Romans used this pigment as ink a lot. The manufacturing procedure consisted on milling and cleaning the earth containing hematite in order to delete the most of impurities and obtain the purer Fe_2O_3 . Like all the earths, also red earth is a very stable pigment, even if in reducing atmosphere its transformation in magnetite ($\text{FeO} \cdot \text{Fe}_2\text{O}_3$, black) can take place; but this transformation happens only above 1000 °C, in case of fires for example [51].

Chapter 4

Degradation of parchment

4.1. Main causes of parchment degradation and structural damage

Natural deterioration of parchment can be caused by internal or external factors. Internal factors depend on the history of the animal from which parchment comes and, especially, on the manufacturing steps. For example, a long soaking in lime can fragment the collagen fibres, making parchment more brittle [43, 59]. External factors are caused by chemical changes due to hydrolysis, gelatinization and oxidation of collagen, promoted mainly by humidity, high temperature, pollutants and biological and microbiological factors (such as bacteria, fungi etc.) [43]. Moreover, parchment degradation can be sometimes accelerated by inks (in particular the acid based ones) and environmental conditions during the centuries of its use, display and storage. Nevertheless, since parchment is a very resistant material, these deterioration processes do not alter significantly its trace elements compositions. Degradation of collagen can take place from the macroscopic level to the nanoscopic one depending on the entity of the damages. Figure 28 shows the different degree of collagen fibres deterioration [39]. At the microscopic level the fibres appear intact with a relative even and smooth surface with signs of helical structure, whereas deteriorated parchment is characterised by frayed and fragmented fibres. At the mesoscopic level it is possible to see the

elementary fibres, well preserved for the new parchment and with a melt like aspect with breaks in the deteriorated one. At the deeper level the fibrils are clearly visible for the new parchment, whereas for the historical one there is no presence of a fibril structure and axial repeat [39].

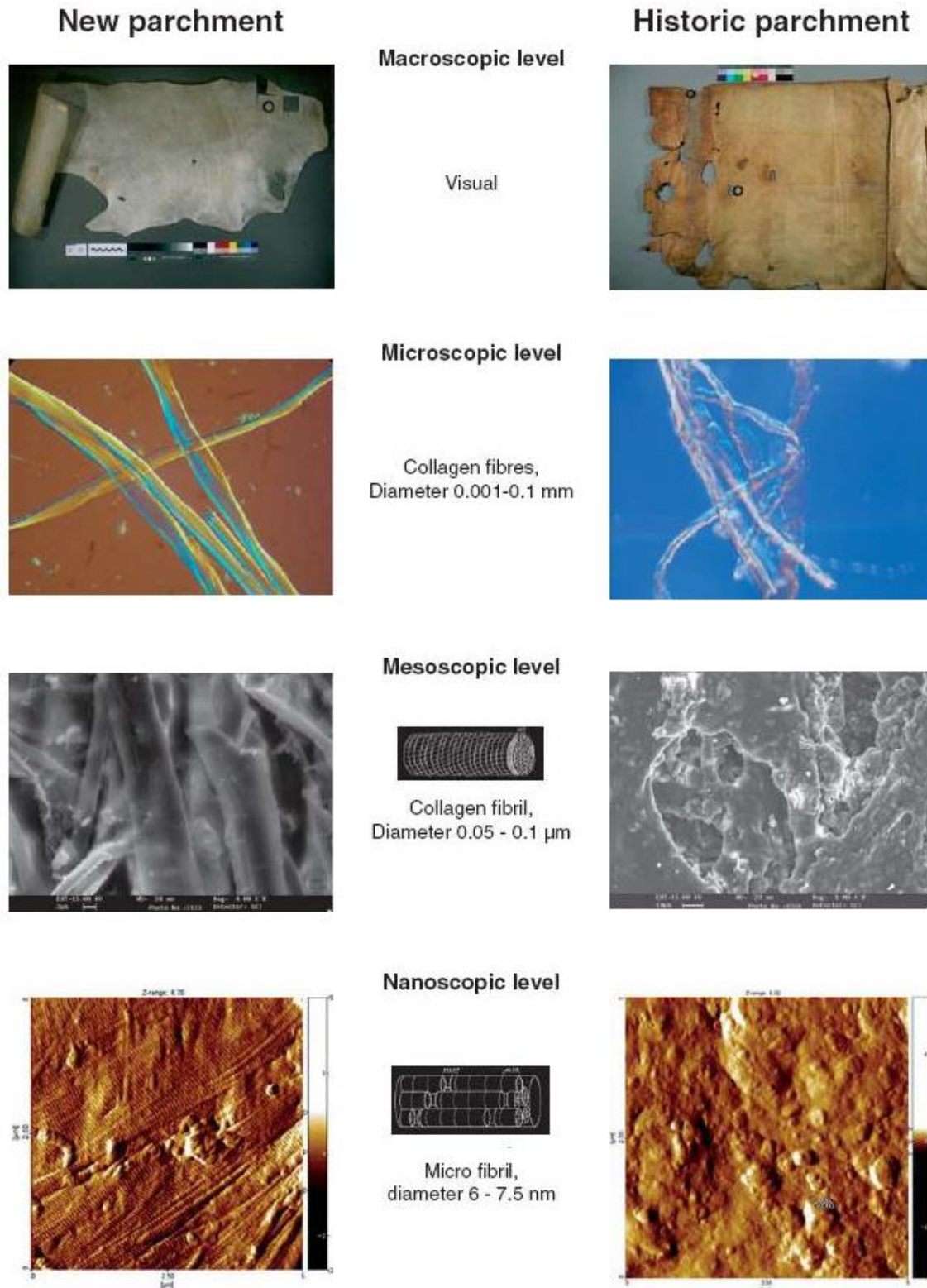


Figure 28. Visualization of new intact and damaged historic parchment at different structural levels [39].

4.2. Influence of humidity and temperature on parchment

The quantity of water inside parchment can influence its properties highly, mainly its stiffness and plasticity: the dimensional variations of parchment depend on the changing of humidity in it. If humidity increases parchment narrows, if humidity decreases parchment dilates. Recent studies have shown that when parchment passes from dry condition to saturated condition (about 95% of relative humidity), it manifests a lengthening variation of about 5%, as it is shown in figure 29 [32].

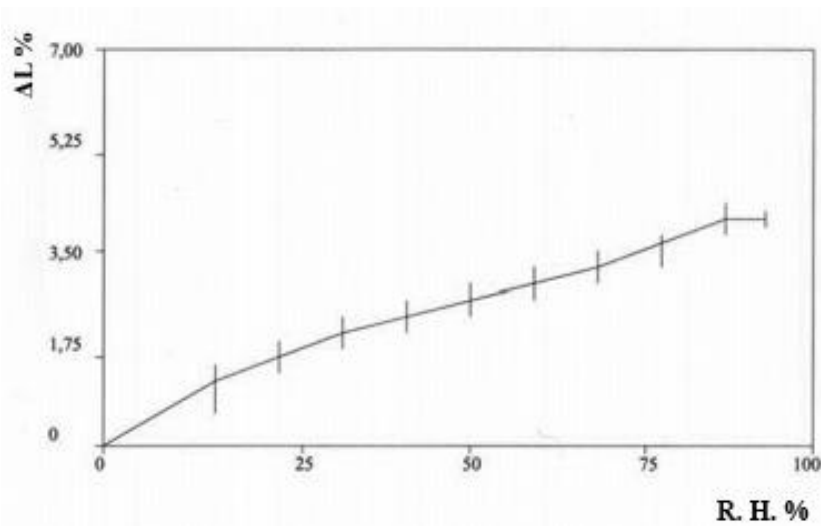


Figure 29. Percentage length variation of parchment samples in response to the change of R.H. [32].

When water becomes part of the collagen structure, it breaks some hydrogen bonds in order to form bonds between fibres. In this way, fibres result less compact and more outdistanced giving more flexibility to the parchment. An increase of the amount of water compacts the fibres allowing establishing inter-fibres hydrogen bonds making the material more rigid with possible folds and deformations [32].

In some cases the gelatinization of proteins can also take place, in particular in very damp and warm conditions. When a high quantity of water is absorbed, a denaturation and aggregation of collagen proteins may occur and lead to the irreversible formation of a heavily hydrated gel matrix, followed by an increase of weight and viscosity [41]. Gelatinization is more likely to occur in partially degraded collagen molecules compared to native intact collagen. In intact collagen, the position, the structure of the peptides and the position of the hydrogen bonds internally in the triple helix make difficult for water to enter and interact in this way. However, if the collagen molecule

is already broken, hydrogen bonds are exposed to the action of water [43]. In the most severe cases, gelatinization can originate the “blocking effect”, the transformation of parchment sheets in contact with each other in a unique compact block [32].

Moreover, high temperatures (above 60-70°C) affect the chemical structure of parchment adversely, leading to a partial or total denaturation of the collagen proteins. This irreversible reaction can transform the native triple helical structure into uncoiled structures and involves an embrittlement of parchment giving rise to a glassy surface of the fibre network, as it is shown in figure 30 [60].

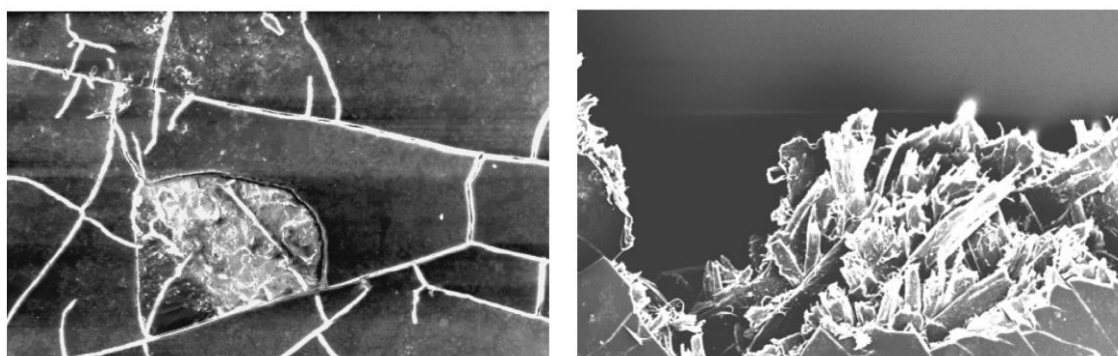


Figure 30. SEM 50 μm magnifications of glassy surface of parchment after heating treatments [60].

A recent study has demonstrated that parchment can resist better to high temperature (40-50 °C) with the presence of humidity (about 60%). In fact, humidity promotes the formation of water bridges and increases intra and inter molecular interactions with a consequent higher stability of collagen fibres [41].

4.3. Influence of UV light and external contaminants on parchment

Although the ancient manuscripts were often stored indoor, also the possible influence of UV light and pollutants have to be considered. UV light, SO_2 and NO_x pollutants, indeed, catalysed by heat, generate easily free radicals, which can oxidize the collagen fibres [41]. The side chains of some amino acids are initially involved, but oxidation can also occur in the backbone of collagen through the rupture of N-C covalent bonds. Especially collagen oxidation reduces the number of

the basic amino acids such as arginine, hydroxylysine and lysine and increases the number of the acidic amino acids such as glutamic acid and aspartic acid. The level of oxidation of collagen in parchment can be assessed by measuring the ratio of basic to acidic amino acids (B/A ratio). In the new collagen this ratio is about 0.70, instead in historic parchment is about 0.5, confirming the oxidative changes [43].

Moreover, atmospheric pollutants, acting with air and humidity, can disrupt the hierarchical structure of collagen catalysing the fragmentations of collagen bonds. Especially SO₂, in presence of humidity (higher than 60%), can lead to the formation of sulfuric acid, able to compromise the material seriously [32].

4.4. Degradation of parchment by inks

First of all it is necessary to underline that parchment is a very resistant material, contrarily to papyrus or paper. The inks described in the previous chapter, generally, do not damage parchment. Also the iron gall ink, known for its high acidity, seems to not degrade parchment. Parchment, in fact, contains a sufficient alkaline reserve deriving from the manufacturing step of soaking in lime. However, by the reaction between gallic acid and iron sulfate, sulfuric acid is developed and sometimes, if it was in high quantity, it could damage superficially the support. In this rare case, the most damages were found only for parchments that suffered a mild soaking in lime. Moreover, for reviving scriptures that tended to discolour, it was common to intervene by spreading a decoction of gallnuts, in order to reform the iron(III)complex. This use was tragic for parchment treated areas that became brownish [32, 46].

Chapter 5

XRF and Raman spectroscopy investigations on ancient manuscripts

5.1. An important find in the Anubis region

In 2007, on the island of Sur above the Fourth Nile Cataract in Northern Sudan (figure 31), a church of the Classic Christian Period, with a rich find of a corpus of medieval manuscripts was discovered by the *Merowe Dam Archaeological Salvage Campaign* [61]. Historians suggest that these manuscripts could be part of the library collection of the 11th century church.



Figure 31. Map of the Sudan with the exact place of excavation circled in white.

Although, greatly crumbled, it represents the most important find of textual material in Nubia in the last years, including exceptional book bindings and leather book covers. The whole find comprises [61]:

- 100 fragments of inscribed parchment;
- a semi-whole parchment *folio*;
- numerous remains of leather bindings with a multitude of decorative elements;
- several texts on folded leather;
- two leather amulet cases, several braided ribbons and one leather object (maybe a sole).

Leather pieces are written in Old-Nubian language, however, parchment samples are written in old Greek. It is possible that the last ones were brought in this area by the early Christians. Both, fragments and *folio* have religious contents.

For this work selected and most representative fragments were chosen for investigations. In total six fragments and the *folio* were analysed by XRF and Raman spectroscopy for the experimental analysis of inks and writing support.

5.1.1. Description of the conditions of the parchment find

The fragments and the *folio*, inscribed on both, flash and hair sides were made from goat or sheep skin and they differ to each other about the quality and the thickness. All the fragments had grubs of insects and they were covered by sand. In some cases, this silicate material became a hard surface-coating layer. Most pieces were also distorted with several tears [61]. The *folio*, instead, seemed in a better state of conservation, with less biological attacks.

5.1.2. Conservation and reconstruction treatments

All the fragments and the *folio* were cleaned with a stiff brush on both sides by a conservator (Mag. Dr. Patricia Engel, European centre for Book and Paper Conservation-Restoration, Donau-University, Krems, Austria). Afterwards they were treated with a cellulose-based product on both sides in order to minimize the distortion. Moreover, this product was used for tear mending and consolidation [61].

Cellulose-based products are soluble polymers, obtained with the substitutions of the –OH groups of cellulose with other groups (e.g. -H, -CH₃, -CH₂COOH) and they are very common consolidants for parchment and generally paper. Many cellulose derivatives, like acethylcellulose and carboxymethylcellulose, were often used on parchment since the beginning of the 20th century. In particular, their use was widespread for brattled parchment caused by the loss of the fat component on the surface. These polymers can confer solidity and softness to parchment, allowing campaigns of conservation-restoration. However, on the other side, these products can give a brownish colour and lucidity to parchment [62].









Due to the different types of ink, front size and line spacing, for some fragments the reconstruction of the text was possible. Six fragments were able to be identified and placed correctly as well as two fragments from the *folio* were replaced in it. Nevertheless, the final reconstruction is not completed yet [61].

5.2. Experimental

5.2.1. Materials

In table 1 and figure 32 the six analysed fragments and the *folio* are shown, respectively.

Table 1. *Rectus* and *versus* of the fragments with their dimensions.

Fragment n°	<i>Rectus</i>	<i>Versus</i>	Dimensions (cm ²)
113+19			6 × 4.5
20			2 × 3.5
5			2.5 × 2.5
92			3.5 × 3.5

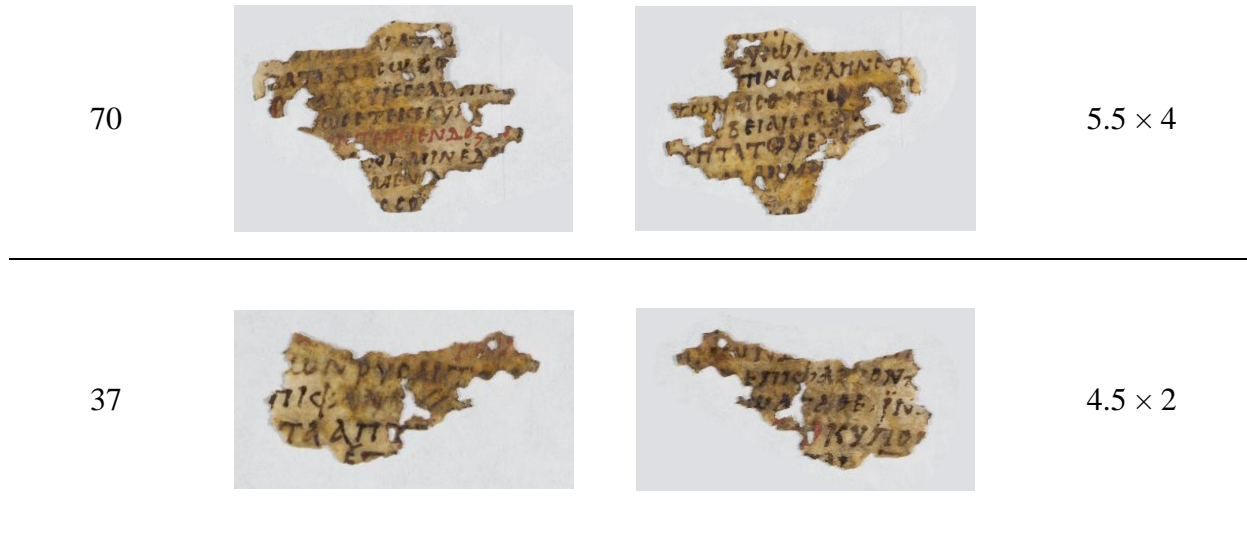


Figure 32. *Rectus* (a) and *versus* (b) of the *folio* (20x24 cm²).

By a first optical analysis it was possible - in the case of the fragments - to distinguish only different types of writings, whereas in the *folio* drawings with the shape of letters, squares and candles can be seen. Moreover, on the *versus* of the *folio* a black cross placed on the right edge was visible.

Black and red inks are used on both, fragments and *folio*. These inks are often used as pure components in the written text, with some exceptions, as shown in figure 33a, where the inks seem to be superimposed. On the *folio* some letters are filled out with red ink in order to get more attraction to the text, as depicted in figure 33b and c.



Figure 33. Red under the black ink of the fragment 20 (a) and black and red decorative letter in the *folio* (b and c), magnification: 16x

Based on the optical examination, the composition of the inks does not seem to be the same when the fragments with the *folio* are compared. The black ink of the fragments, in fact, is more brownish and the red one appears more orange, as shown in figure 34.

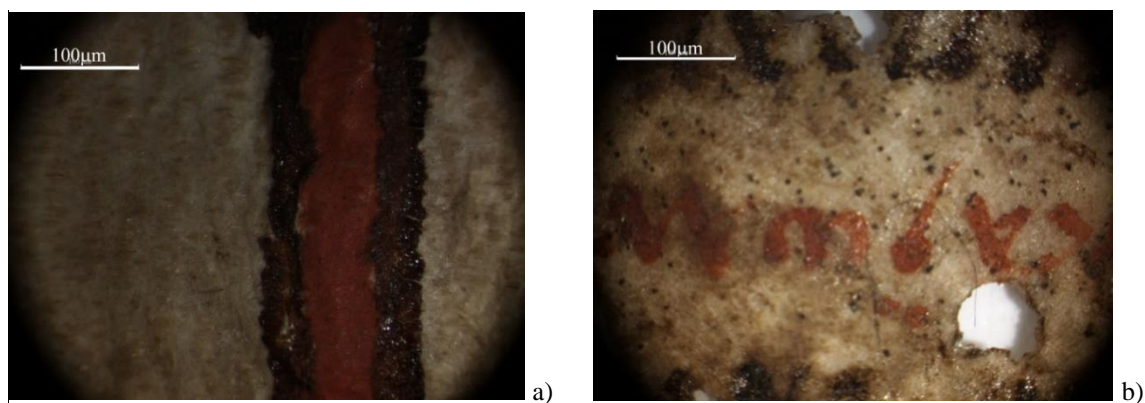


Figure 34. Red ink on the *folio* (a) and red ink on fragment 113+19 (b). The second one is more orange than the first one, magnification: 16x

Moreover, the black ink used for the cross placed on the right edge of the *folio* (figure 32), seems to be different from the ink used in the text. It is darker and its texture is similar to a powder.

5.2.2. State of conservation

Considering that both fragments and *folio* have undergone the same consolidation treatment, they are in a different state of conservation. Fragments are mainly characterized by clear gaps and the parchment is very brittle and tends to crumble easily. There are many dark-brown spots, shown in figure 35, which could be due to the presence of bacteria or moulds grown in humid environment. Moreover, there are particular stains that could be caused by the iron gall ink degradation pathways due to the acidic component of the ink. These stains can be caused by two main factors. They could arise from a thick layer of ink of the verso written text, because of the

ink absorption by the parchment, or they could be due to the common ancient practice to add a decoction of gallnuts when the fading of the iron gall ink occurred [46].

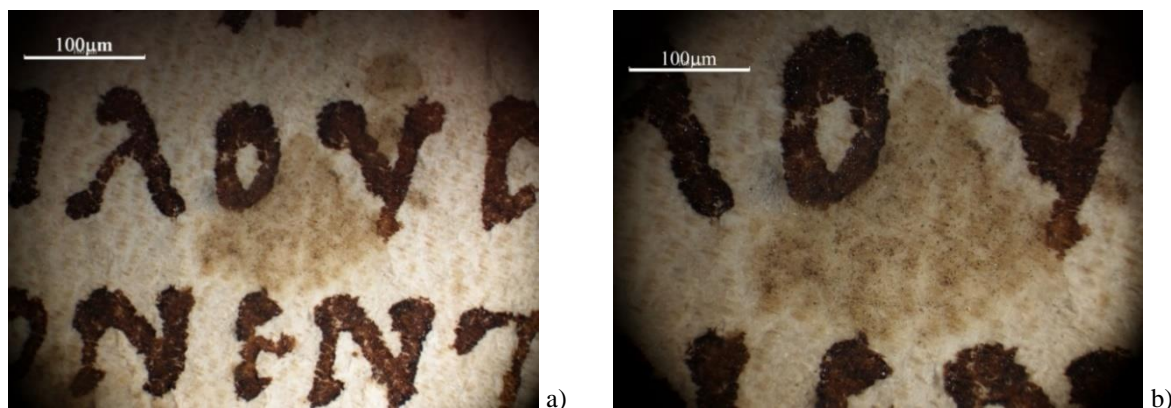


Figure 35. Dark spots on parchment, magnification: 16x (a) and 24x (b).

Black and red inks, however, compared to the parchment, seem to be in a relatively humble state of conservation, characterized mainly by ink fading.

For what concern the *folio*, it is possible to see that the inks are in a very good state of conservation, without a clear fading. About the support, instead, there are only some dark little stains, probably caused by moulds or bacteria. Moreover, parchment is less brittle the one of the fragments.

On both fragments and *folio*, yellowish and glossy areas are visible. Those areas are characterized by a heterogeneous *patina*, probably formed after the conservation treatment with the cellulose-based material, as shown in figure 36. This sort of coating is more evident and thicker on the crumbled areas.

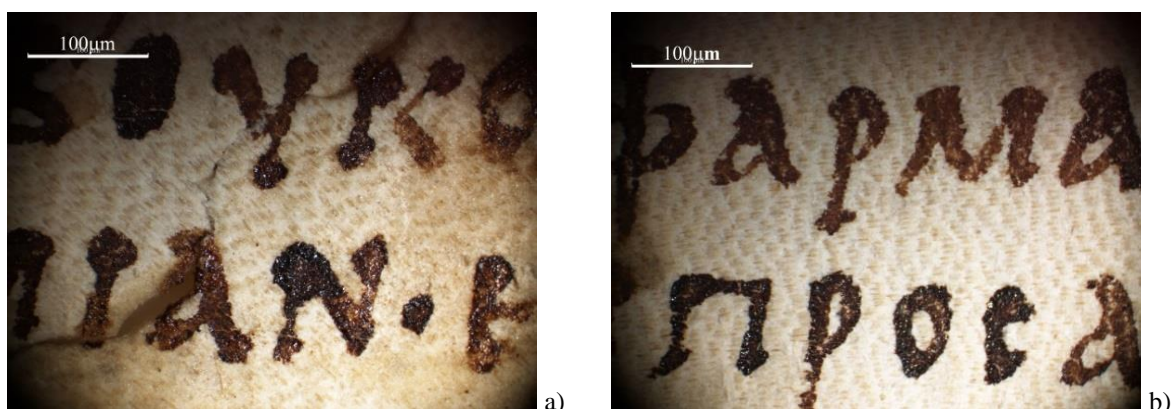


Figure 36. Comparison between the yellowish *patina* on crumbled area (a) and no crumbled area (b) of the *folio*.

5.2.3. Methods

For all the objects (fragments and *folio*) XRF and Raman analyses were performed on parchment as well as on inks. The evaluation was based on the comparison of the acquired data with reference spectra of the ISTA database (Institute of Natural Sciences and Technology in Art) previously obtained. Moreover, the ancient parchment composition was compared with a new and not damaged one, prepared by traditional methods at the School of Conservation, Royal Danish Academy of Fine Arts (Copenhagen) and the Dutch parchment craftsman Z.H. de Groot.

XRF and Raman analyses were carried out using the instruments already described in sections 1.2.5 and 1.3.5.

5.3. Results and discussion

5.3.1. XRF

On the fragments

The samples of the ancient fragments are richer in elements than the reference one (showing only Ca), as can be seen in table 2, due to the accumulation of contaminants through the centuries. Generally, the main elements detected on the **parchment** were Ca, Si, Fe, K, and Cl, as shown in the tables 3-8. The presence of calcium derives from the manufacturing treatment of the parchment with $\text{Ca}(\text{OH})_2$ (as described in section 2.3.2). The presence of Si and Fe can be attributed to soil and dirt, as the fragments were buried before the excavation. Furthermore, Fe can also derive from iron-based inks probably used in the text (such as iron gall ink or red earth ink) which were partly absorbed by the support due to the writing vehicles. Low values of K are intrinsic of the parchment support, whereas high values can be attributed to the presence of soiled earth too or caused by the presence of moulds or bacteria. K could be also imputable to the carbon black ink probably used in the text obtained from potassic plants which could be absorbed by the parchment support. Moreover, this element can be due to the presence of the cellulose-based product applied on the parchment surface during the consolidation treatment. Cellulose-based products, in fact, are easily attacked by moulds, which produce potassium after their life cycle.

Furthermore, the elemental distribution of K on the samples was very heterogeneous. In fact, in some darker parchment areas (called “*patina*” in the tables 6-8), high concentration of K was detected whereas in some objects K was not detectable. Nevertheless, it was possible to understand that no correlation was evident between the thickness of the cellulose-based consolidant and the concentration of K. Therefore, it was possible to assume that, despite a small amount of K which is intrinsic in the parchment, its concentration and distribution could vary depending on the presence of biological agents. Interestingly, also Cl was observed in all the samples, probably due to atmospheric pollutants.

Table 2. Comparison between the XRF results of the parchment fragments with the reference ones.

Qualitative analysis of the parchment fragments	Qualitative analysis of the reference parchment
Si, Cl, K, Ca, Fe	Ca

The results of the investigations on the **black/brown and red inks** (figures 37-42 and tables 3-8) showed the presence of the elements Fe and Pb. Especially the high amount of Fe (around 1000 counts in comparison with 350-450 counts for the parchment) could be related to the iron gall ink applied for the brown-black text (fragments 113+19, 20, and 5), as well as for the red-earth based ink used for the red writings of fragments number 70 and 37. Lead-based red inks, inferred from the presence of Pb, were found in fragments 113+19, 20, 5 and 92. Moreover, it is necessary to underline that a mixture of red lead and red-earth could be used in fragments 113+19, 20 and 5, since a high amount of iron was found in the red ink. The black ink of fragments 92, 70 and 37 was characterized by a low Fe content (about 400 counts, similar to the parchment). It is therefore likely that for these samples no iron gall ink was applied. For a better identification of this ink, Raman spectroscopy was chosen as a complementary technique.

Where possible, for the XRF analysis, spots on writings without any text on the back side were chosen, because of the high penetration of the X-ray radiation. In tables 3-9 only the elements with higher intensities/counts in comparison to the parchment are presented.

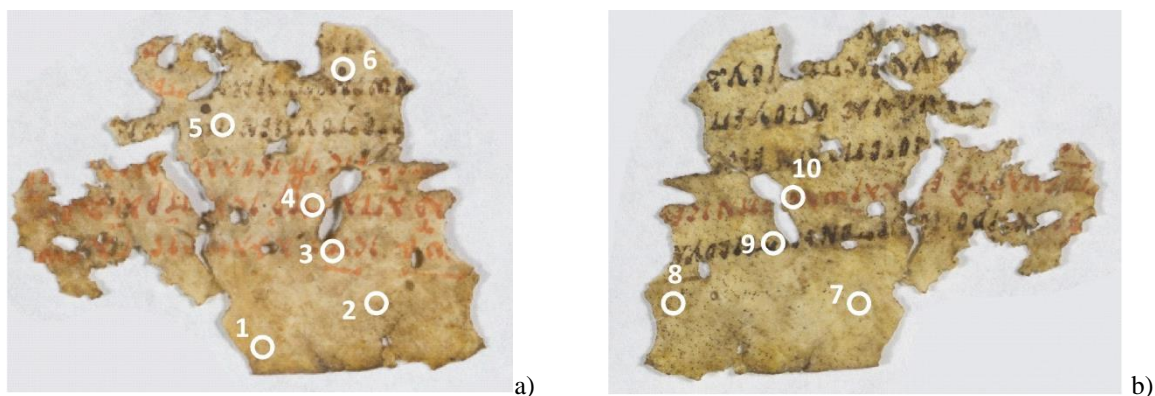


Figure 37. Analysed spots (circled in white) of fragment 113+19 *rectus* (a) and *versus* (b).

Table 3. XRF results of the analysed spots (circled in white) of the fragment 113+19 *rectus* and *versus*. The elements in bold are the main elements, whereas the elements in brackets are of minor content.

Analysed spots	Description	Qualitative analysis
1	Parchment	Si, Cl, K, Ca, Fe
2	Parchment	Si, Cl, K, Ca, Fe
3	Red ink	(Si), Fe, Pb
4	Red ink	Si, Ca, Fe, Pb
5	Black ink	(Si), K, Fe
6	Black ink	Si, K, Ca, Fe
7	Parchment	Si, Cl, K, Ca, Fe
8	<i>Patina</i> on parchment	(Ca), Fe
9	Black ink	(Si), Fe
10	Red ink	Si, Ca, Fe, Pb

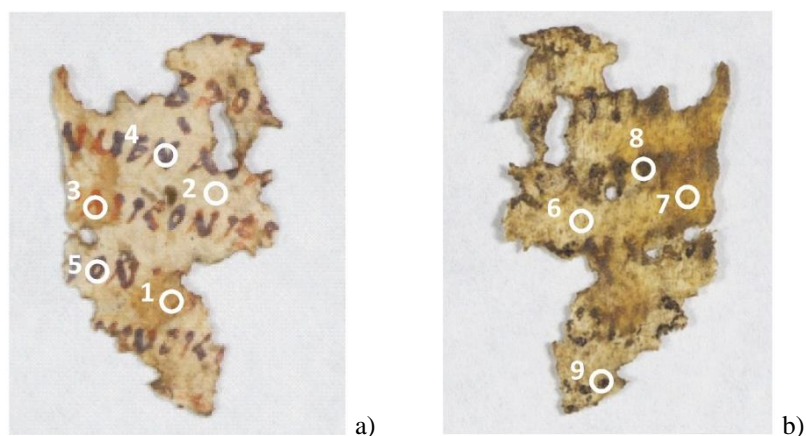


Figure 38. Analysed spots (circled in white) of fragment 20 *rectus* (a) and *versus* (b).

Table 4. XRF results of the analysed spots (circled in white) of the fragment 20 *rectus* and *versus*. The elements in bold are the main elements, whereas the elements in brackets are of minor content.

Analysed spots	Description	Qualitative analysis
1	<i>Patina</i> on parchment	K
2	Parchment	Si, Cl, K, Ca, Fe
3	Red ink	(Cl), K, Fe, Pb
4	Red + black ink	(Si), (Cl), K, Fe, Pb
5	Black ink	Si, (Cl), K, Ca, Fe
6	Parchment	K, Cl, Ca, Si, Fe
7	<i>Patina</i> on parchment	Si, K
8	Black ink	K, (Ca), Fe
9	Black ink	(Cl), (K), (Fe)

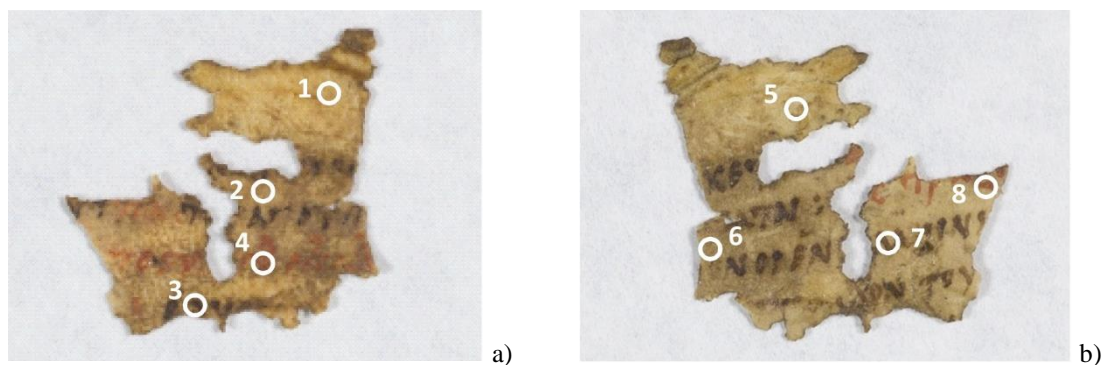


Figure 39. Analysed spots (circled in white) of fragment 5 *rectus* (a) and *versus* (b).

Table 5. XRF results of the analysed spots (circled in white) of the fragment 5 *rectus* and *versus*. The elements in bold are the main elements, whereas the elements in brackets are of minor content.

Analysed spots	Description	Qualitative analysis
1	Parchment	Si, Cl, K, Ca, Fe
2	<i>Patina</i> on parchment	K, Cl, Fe
3	Black ink	Si, Fe
4	Red ink	(Si), K, Fe, Pb
5	Parchment	Si, Cl, K, Ca, Fe
6	<i>Patina</i> on parchment	K, Ca, Fe
7	Black ink	K, Fe
8	Red ink	Fe, Pb

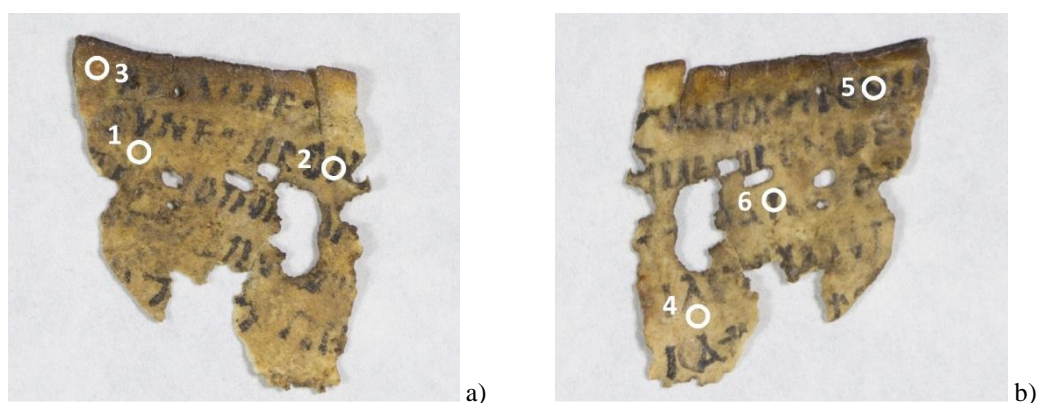


Figure 40. Analysed spots (circled in white) of fragment 92 *rectus* (a) and *versus* (b).

Table 6. XRF results of the analysed spots (circled in white) of the fragment 92 *rectus* and *versus*. The elements in bold are the main elements, whereas the elements in brackets are of minor content.

Analysed spots	Description	Qualitative analysis
1	Parchment	Si, Cl, K, Ca, Fe
2	Black ink	(Si)
3	Red ink	Pb
4	Parchment	Si, Cl, K, Ca, Fe
5	Black ink	No difference from n° 1, 4
6	Black ink	No difference from n° 1, 4

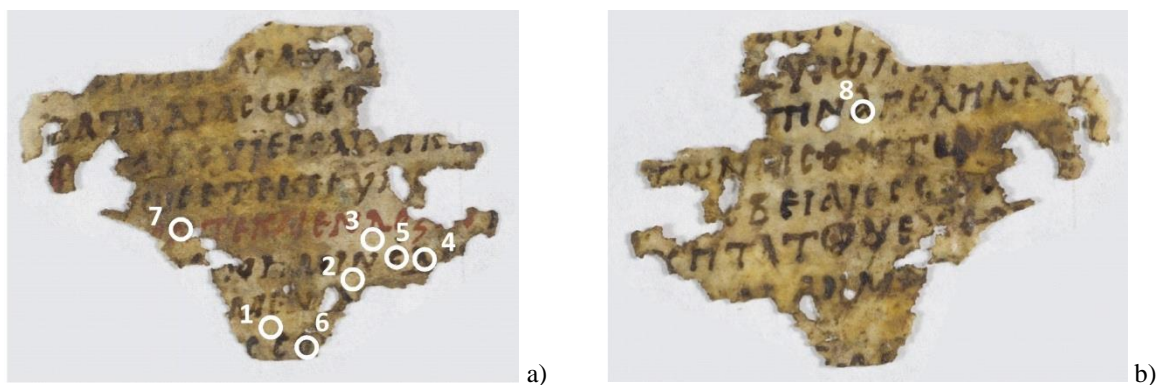


Figure 41. Analysed spots (circled in white) of fragment 70 *rectus* (a) and *versus* (b).

Table 7. XRF results of the analysed spots (circled in white) of the fragment 70 *rectus* and *versus*. The elements in bold are the main elements, whereas the elements in brackets are of minor content.

Analysed spots	Description	Qualitative analysis
1	Parchment	Si, Cl, K, Ca, Fe
2	Parchment	Si, Cl, K, Ca, Fe
3	Parchment	Si, Cl, K, Ca, Fe
4	Black ink	No difference from n° 1-3
5	Black ink	(Si), K , Ca, Fe
6	Black ink	K , Fe
7	Red ink	Si, K , (Ca), Fe
8	Black ink	No difference from n° 1-3

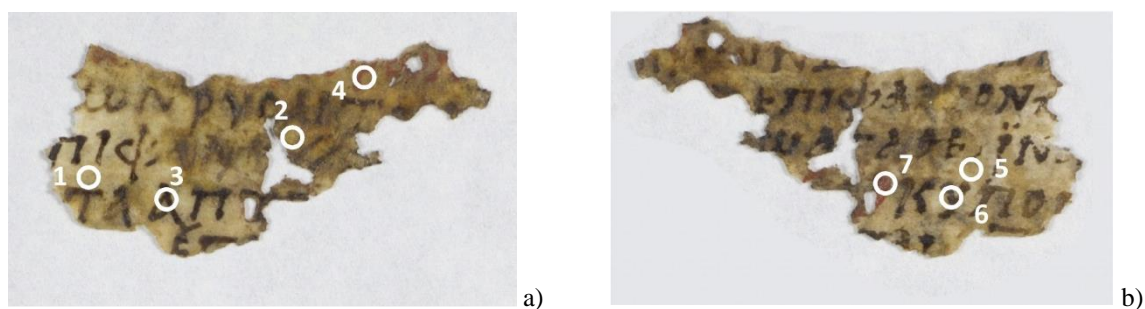


Figure 42. Analysed spots (circled in white) of fragment 37 *rectus* (a) and *versus* (b).

Table 8. XRF results of the analysed spots (circled in white) of the fragment 37 *rectus* and *versus*. The elements in bold are the main elements, whereas the elements in brackets are of minor content.

Analysed spots	Description	Qualitative analysis
1	Parchment	Si, Cl, K, Ca, Fe
2	<i>Patina</i> on parchment	Si, K , Ca, Fe
3	Black ink	(K), Ca
4	Red ink	Si, K, Ca, Fe
5	Parchment	Si, Cl, K, Ca, Fe
6	Black ink	No difference from n° 1, 5
7	Red ink	K , Fe

On the folio

The results of the composition of the **parchment** are similar to the ones of the previously described fragments, showing Ca deriving from the manufacturing treatments with $\text{Ca}(\text{OH})_2$ and Si, K, Fe and Cl as constituents of the parchment or - as described already – probably deriving from the soil, moulds, inks or contaminants in general.

Compared to the fragments, interesting differences in the **ink** compositions were found (figure 43 and tables 9). The presence of Hg and S in the red ink clearly indicates the presence of vermilion. The black ink, instead, is probably carbon-based ink, because the total amount of iron

in the black spots did not show a big difference in comparison to the parchment. Also the black cross drawn on the *rectus* side does not show any Fe content.



Figure 43. Analysed spots (circled in white) of the *rectus* (a) and *versus* (b) of the *folio*.

Table 9. XRF results of the analysed spots (circled in white) of the *rectus* and *versus* of the *folio*. The elements in bold are the main elements, whereas the elements in brackets are of minor content.

Analysed spots	Description	Qualitative analysis
1	Parchment	Si, Cl, K, Ca, Fe
2	Red ink	S, Hg
3	Red ink	S, Hg
4	Black ink	Cl, K, Ca, Fe
5	Black ink	Cl, K, (Ca), Fe
6	Black ink	Cl, Ca, Fe
7	Black ink	Cl, K, Ca, Fe

5.3.2. XRF elemental mapping

In order to get a better understanding of the used inks, XRF imaging investigations were performed. As described in section 1.2.5 an area of interest was selected to get an elemental distribution. With this modality it was possible to visualize the different concentrations of the detected elements by creating a false-colour image of the selected area.

On the fragments

The elemental mapping (figure 44) was performed on the *versus* of fragment 70 with 1 second per step of acquisition time, in order to estimate the distribution of the elements and confirm the first XRF investigation obtained by spot analysis. In these mapping images, each colour is related to a specific element: red for Fe, green for Ca and blue for K, with the colour brightness related to the counts. Therewith it was possible to correlate the XRF spectrum with a false-colour image. It was possible to see that the black ink is not a Fe based ink, as in the area corresponding to the black writing only the presence of K and Ca was detected. Fe was only present in the red writing, confirming that this ink is a red earth-based ink. This result is supported also by the absence of other elements, such as lead or mercury, typical of other red inks. The absence of iron in the black ink is indicative of the possible use of a carbon-based material. In fact, vegetal carbon black was the typical black ink used on parchment in that period.

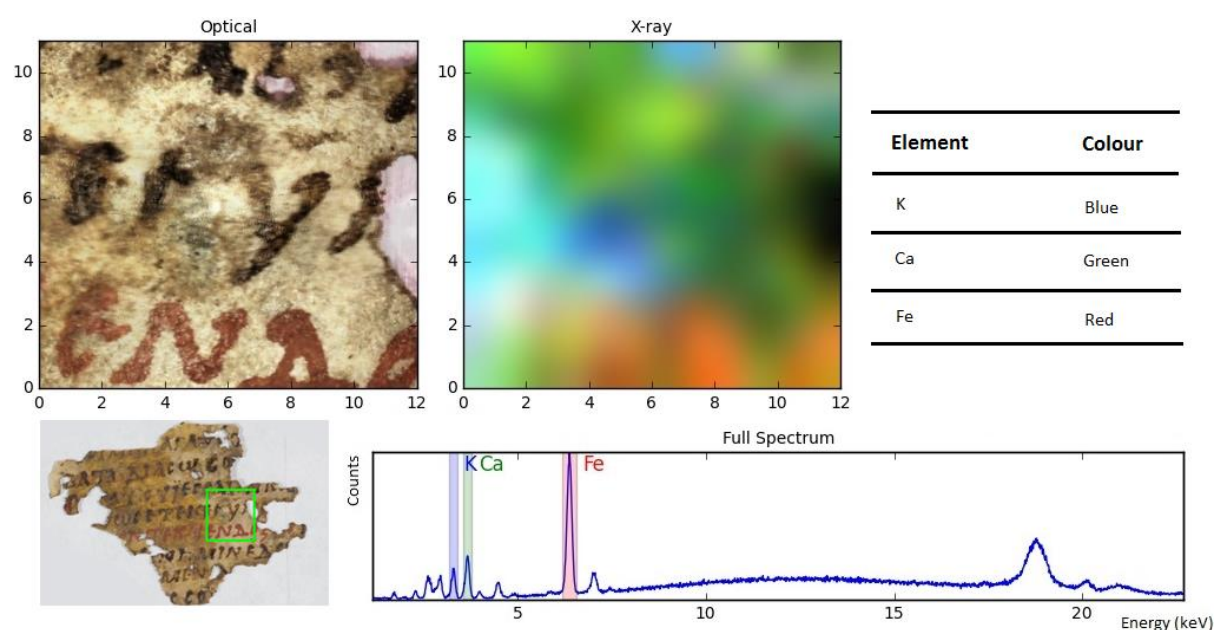


Figure 44. Selected area for the mapping of the *versus* of fragment 70. The imaging and the spectrum show the presence of K (blue), Ca (green) and Fe (red).

Furthermore, as it is possible to observe in the three mapping images, everyone of a single element (figure 45), differently from the previously map, here the false-colour is related to the elemental concentration of Ca, Fe and K: from the highest values represented in red to the lowest values in blue, through the whole palette of visible light. For example, iron is high in correspondence to the red ink, suggesting to be an iron-based red ink (e.g. red earth).

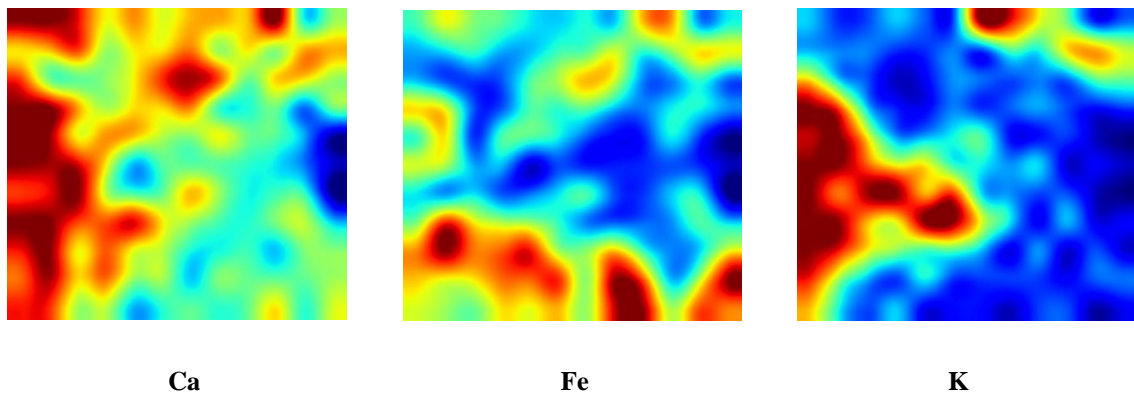


Figure 45. Mapping image of Ca, Fe, and K of the *versus* of fragment 70 as in figure 44. Red colour is referred to a high content of the elements, whereas the blue shows a low content.

For the same fragment, a second attempt of imaging for the estimation of the elemental distribution was performed. Therefore, only the red ink area was selected (figure 46) in order to confirm the presence of a red earth pigment in the ink. In this case, the acquisition time was increased to 10 seconds per step allowing a more reliable detection of the elements. The final results are shown in the imaging picture (the colour codes are the same of the map in figure 44), where the red ink could be identified definitely as red earth pigment.

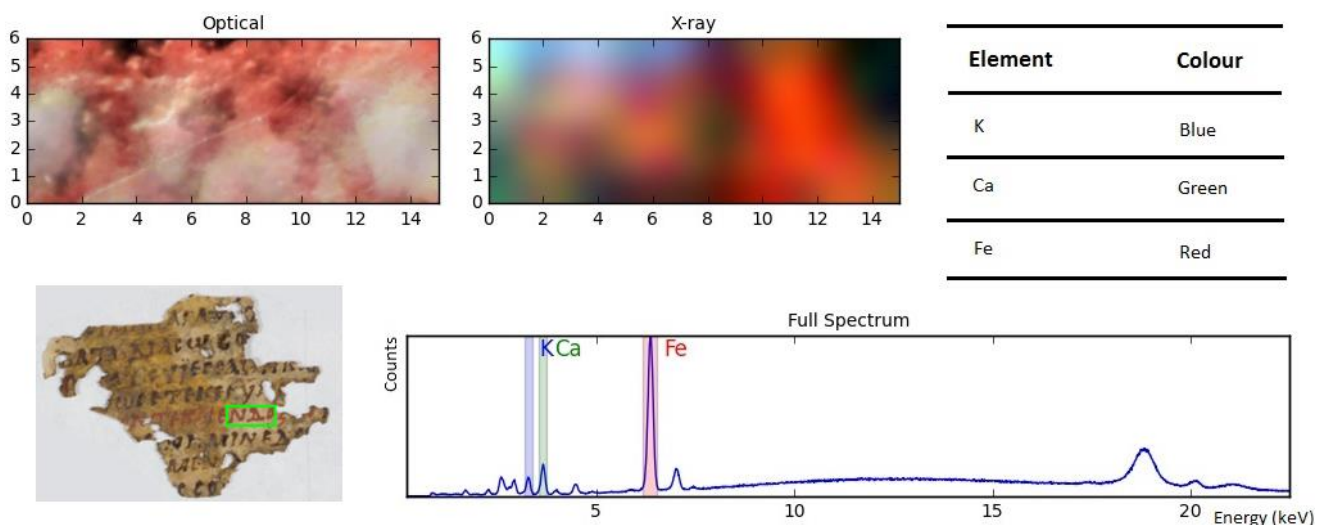


Figure 46. Selected area for the mapping of the *versus* of fragment 70. The mapping and the spectrum show the presence of K (blue), Ca (green) and Fe (red).

A study concerning the homogeneous distribution of the elements present in the parchment was performed. It was possible to detect high intensities of Ca and K in some areas, as shown in figure 47. The red ink area shows only a high content in Fe and no calcium or potassium.

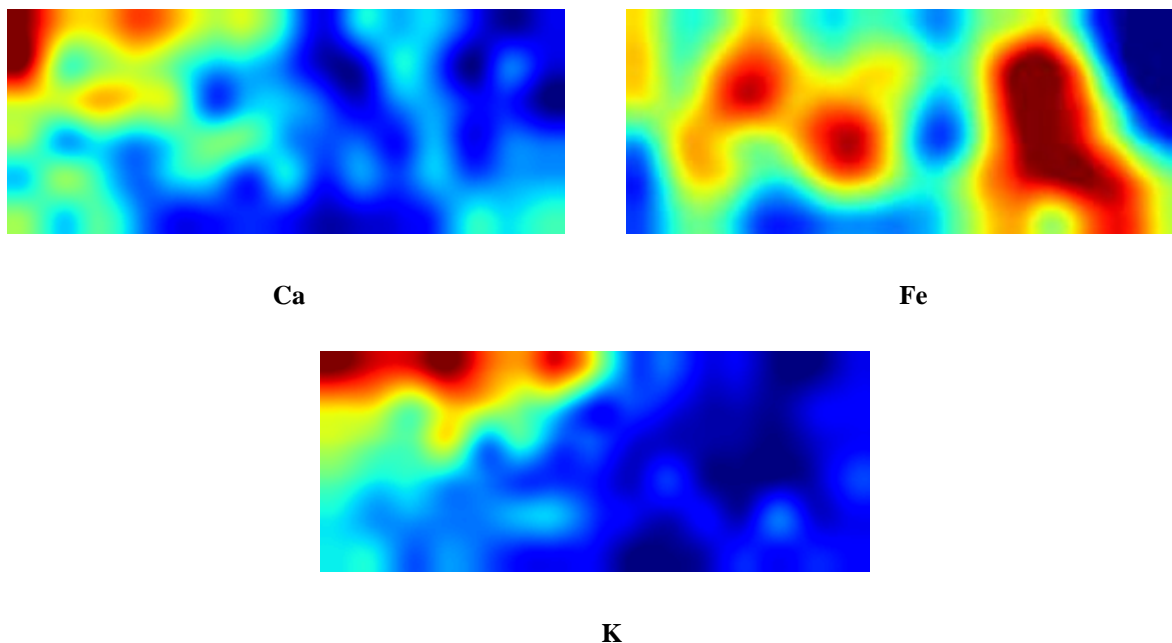


Figure 47. Mapping image of Ca, Fe and K of the *versus* of fragment 70 as in figure 46. Red colour is referred to a high intensity of the elements, whereas the blue shows a low contents (amount).

On the folio

The mapping of the *folio* was performed with 10 seconds per step of acquisition time in order to study the distribution of the main elements. As shown in figure 48, the elements detected were K, Cl and Hg, confirming that for the red ink vermillion was applied.

As it is possible to see in figure 48, black ink was characterized by the absence of Fe. Therefore, as already described for the fragments, the use of carbon-based black ink could be assumed.

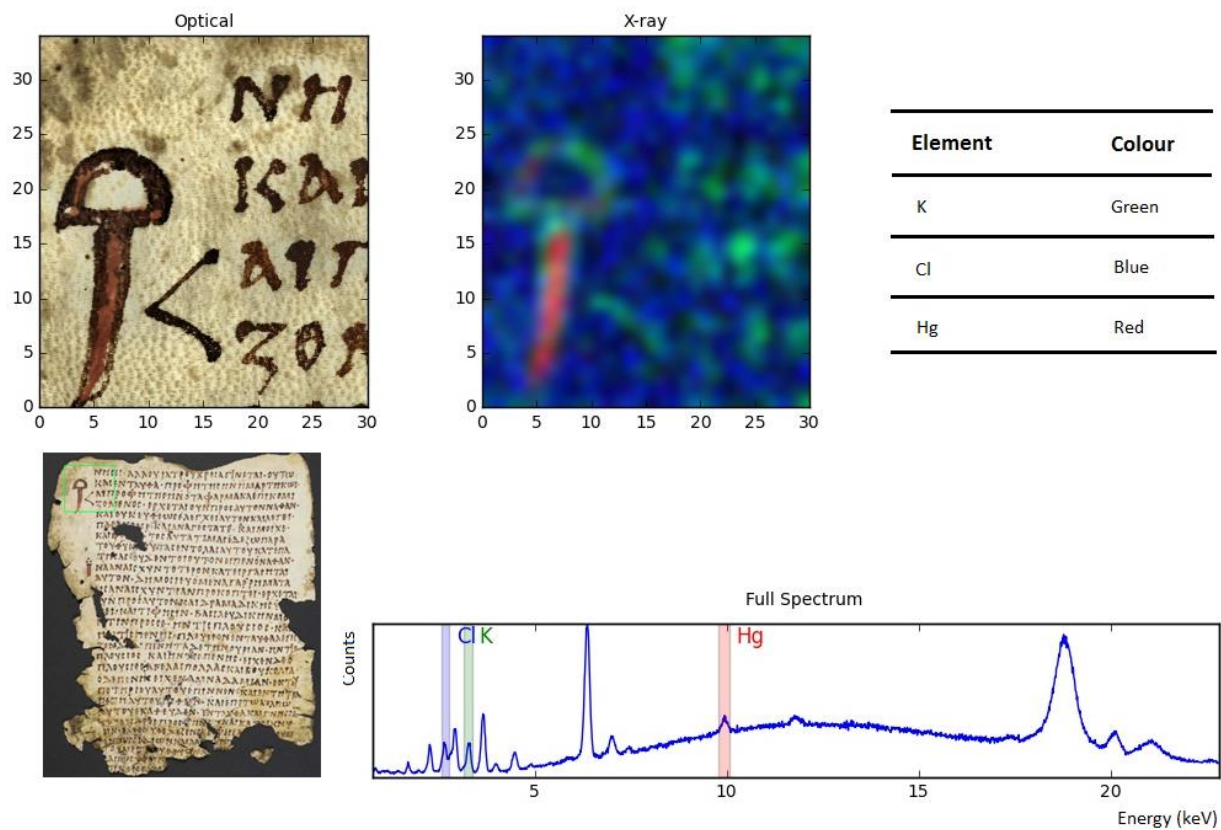


Figure 48. Selected area for the elemental mapping of the *rectus* of the *folio*. The images and the spectrum show the presence of Cl (blue), K (green) and Hg (red).

Some investigations concerning the distribution of elements in the writing and parchment were performed (figure 49). The presence of Hg and the very low level of Fe confirmed that the red ink is vermilion (cinnabar-based), as already discussed. Ca was heterogeneously distributed in the parchment and in particular on the dark stains, maybe as calcium oxalate from moulds or bacteria. K, instead, appeared higher in the writings than in the parchment; this could be due to the use of carbon from potassic plants.

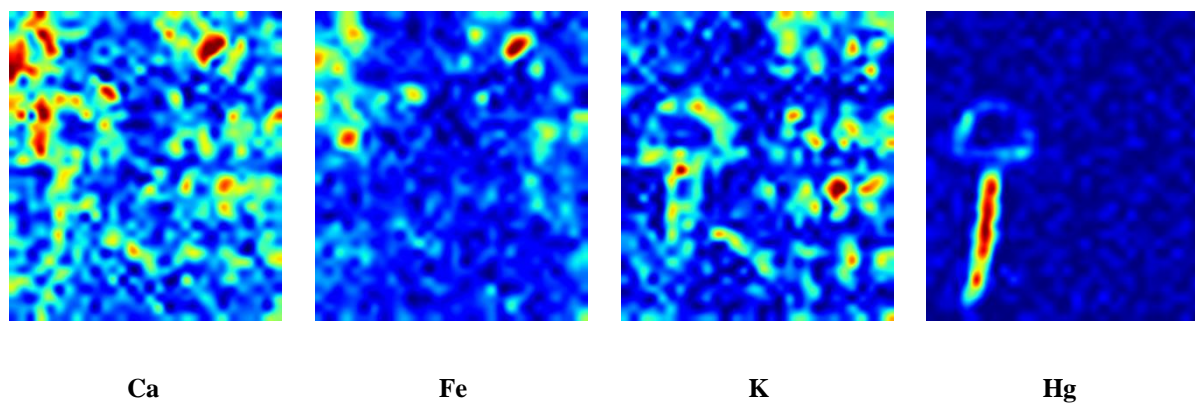


Figure 49. Mapping of Ca, Fe, K and Hg of the *rectus* of the *folio* in figure 48.

In summary: XRF spot analysis and elemental mapping revealed that the inks used on fragments 113+19, 20 and 5 were iron gall ink for the black/brown inks and lead red or a mixture of red lead with red earth for the red ink. For fragments 70 and 37, the black/brown ink used was indirectly identified as a carbon-based ink; the red, instead, was identified as a red earth. Moreover, the black ink of fragment 92 was carbon-based and the red one was recognised as red lead. Finally, in the *folio* the black ink was identified as a carbon black, whereas the red/orange one was identified as vermilion.

5.3.3. Raman

Raman spectroscopy allows to distinguish between pigments or inks of the same or very similar colour by studying their diverse structural properties [12]. In particular, it can be useful to distinguish between iron gall and carbon black as well as between vermilion, red lead and red earth inks for the red pigments and inks.

Measurements were carried out on the same analysed spots chosen for the XRF measurements.

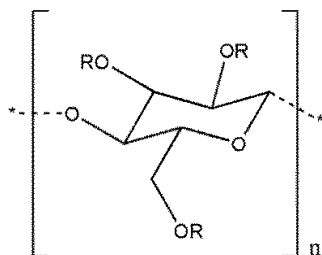
However, particular attention has to be paid to the thermal degradation of the pigments caused by the laser power. In our case, measurements were performed with the 785 nm laser keeping the power/time exposure set-up as low as possible.

The previous restoration treatment caused a high difficulty in collecting the Raman spectra as well as in their interpretation. In order to improve physical properties related to durability and conservation of the artefacts, restorers swabbed on the fragments an inhomogeneous coating layer of cellulose-based consolidating material. These organic compounds, unluckily, showed the main Raman active vibrations in the same range of parchment and black and red inks, resulting superimposed.

A few investigations had to be carried out on pure consolidating materials prior to the Raman measurements of fragments and the *folio*.

Investigation on the cellulose-based consolidating materials

Three cellulose-based materials widely used for parchment and paper consolidation were chosen: Culminal MC 40, Klucel G and Tylose MH 300. The first one is a methylcellulose based material, the second one hydroxypropylcellulose, and the last one methylhydroxyethylcellulose based. Their molecular structures are shown in figure 50.



-Methylcellulose: R = H or CH₃

-Hydroxypropylcellulose: R = H or (CH₂CHOCH₃)_nH

- Methylhydroxyethylcellulose: R = H or CH₃ or (CH₂CH₂O)_n

Figure 50. Molecular structure of cellulose monomer.

The comparison between the spectra of the different cellulose-based products is presented in figure 51, showing that the spectra of the consolidating products are very similar to each other.

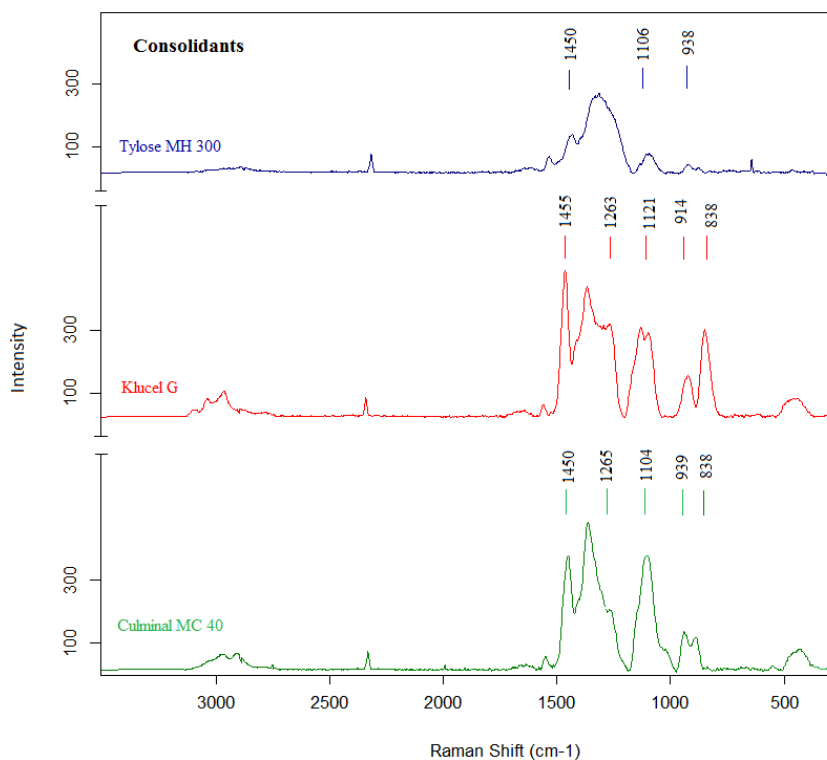


Figure 51. Raman spectra of Culminal MC 40 (green), Klucel G (red) and Tylose MH 300 (blue).

Usually, the most important molecular information about cellulose comes from vibrational signals between 1500 and 200 cm^{-1} . The peak around 1450 cm^{-1} is due to the vibration of CH_2 in an amorphous matrix. The shoulder at around 1265 cm^{-1} is due to the CH_2 twisting [62] and the peak around 1100 cm^{-1} is due to the COC stretching. Moreover, between 890 and 935 cm^{-1} the HCC and HCO bending are visible. [62, 63].

Broader signals in the spectra of cellulose-based products, as in the case of Tylose, suggest a stronger amorphous character of this material [5, 6].

Moreover, in figures 52 and 53, the comparison between one of the cellulose-based materials, Culminal MC 40, with the parchment spectrum of the *folio* and with an iron gall ink reference spectrum is presented, where the masking effect caused by the consolidating material is clearly visible.

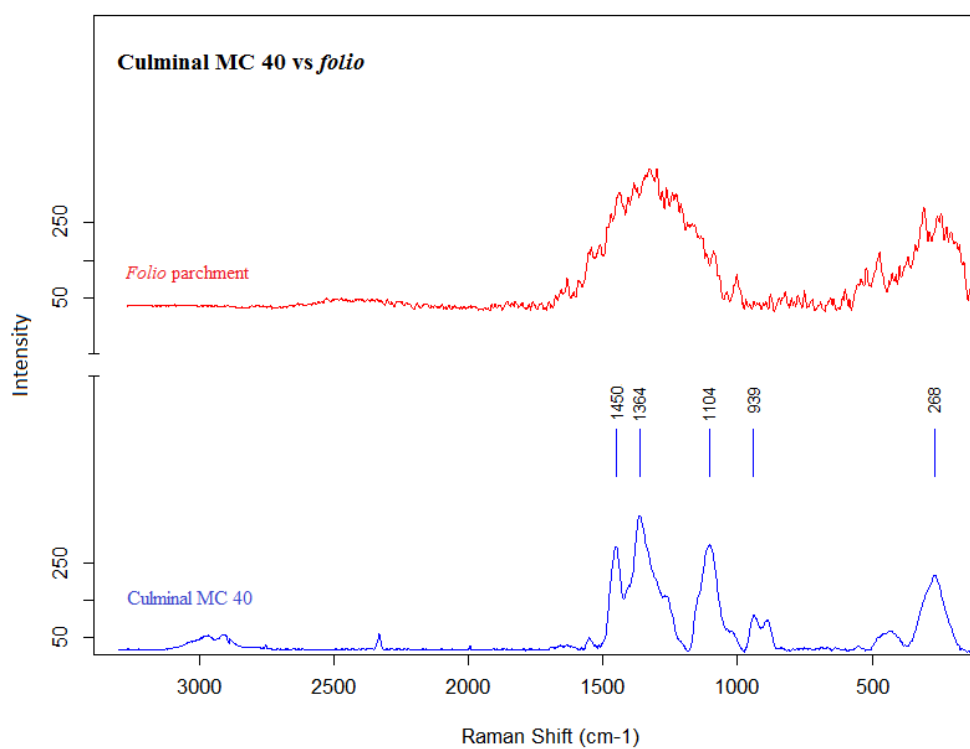


Figure 52. Raman spectrum of Culminal MC 40 (blue) in comparison with the parchment spectrum of the *folio* (red).

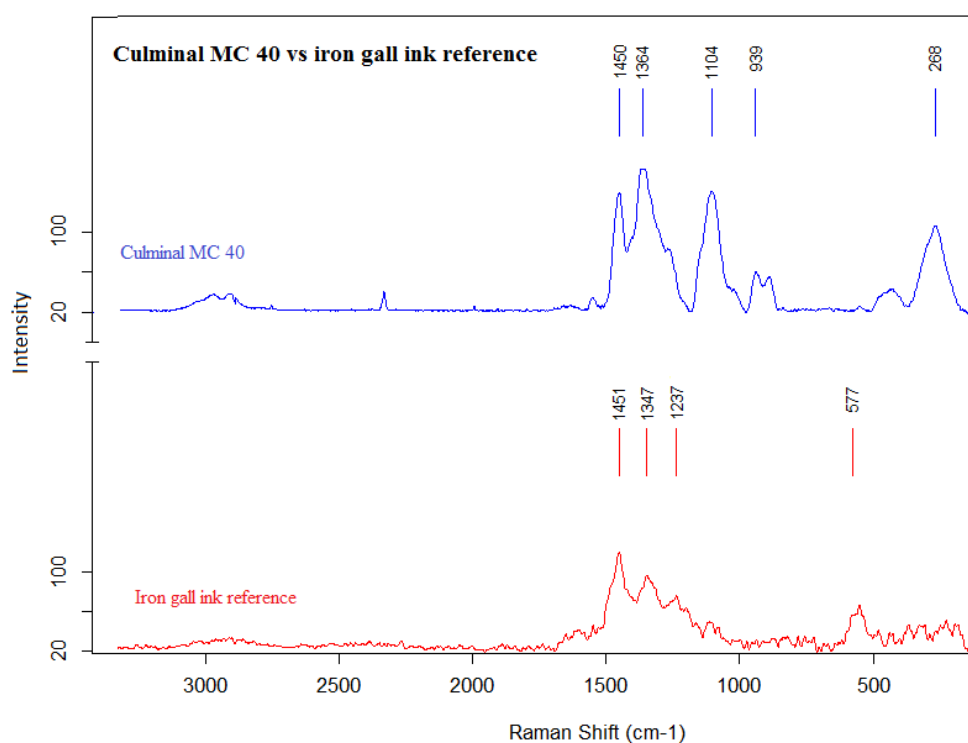


Figure 53. Raman spectrum of Culminal MC 40 (blue) in comparison with iron gall ink reference spectrum (red).

Moreover, it cannot be excluded that the presence of organic materials on the surface can cause micro-burns due to the power of the laser. Although no damaging of the parchment support occurred, the superficial micro-burns (not visible with the naked eye) yields to an increase of the carbon signal. Carbon depicts two broad bands in the range of 1200-1600 cm⁻¹ in the Raman spectra [29], which can create artefacts hiding signals of the analysed material with consequent loss of information.

Investigation on the parchment

The first analytical approach was performed on the writing support. Raman spectra of the parchment of both, fragments and *folio* were acquired and compared with the reference spectrum of new parchment (prepared by traditional methods at the School of Conservation, Royal Danish Academy of Fine Arts (Copenhagen) and the Dutch parchment craftsman Z.H. de Groot).

The spectrum of the new parchment used as reference (figure 54 and 55) depicts the typical bands of collagen. At 1665 cm⁻¹ there is the amide I peak, mainly due to the C=O stretching vibration. At 1552 cm⁻¹ there is the amide II band characterized by 60% of N-H bending and 40% of C-N stretching. At 1470 cm⁻¹ the C-H aliphatic bending vibrations can be seen and around 1243

cm^{-1} the amide III peak, due to 30% of N-H bending and 40% of C-N stretching is present. The amide III-band is the more complex vibration that involves several atoms in the peptide backbone [29, 30].

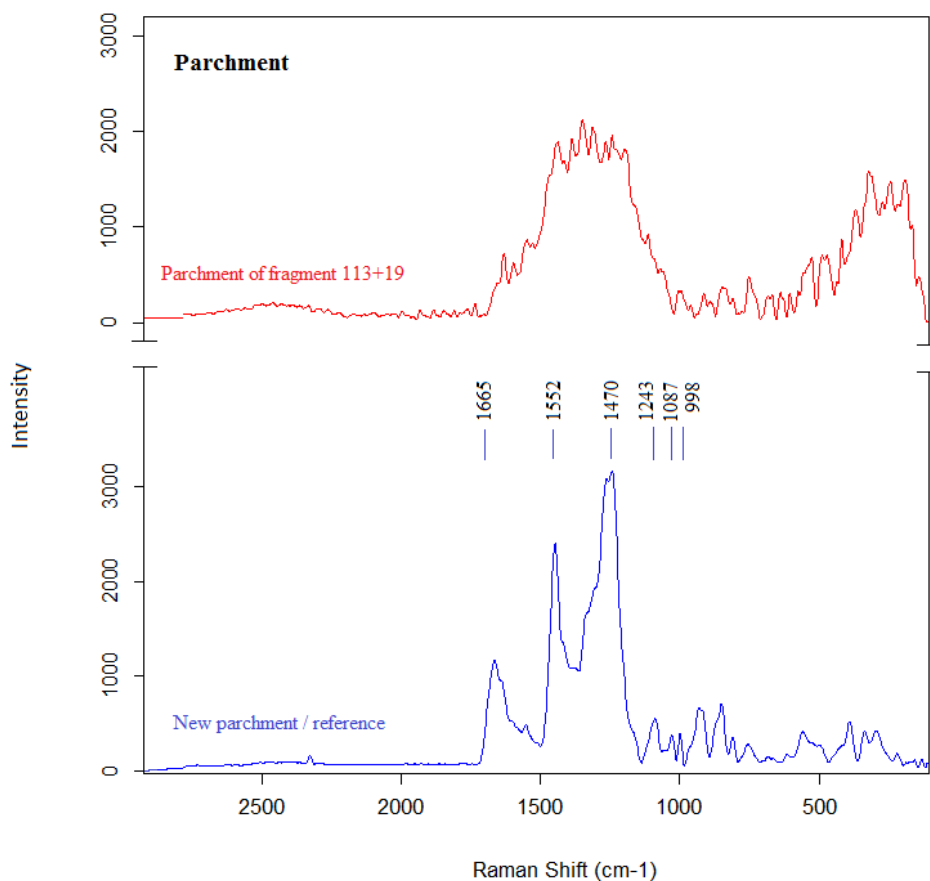


Figure 54. Raman spectrum of the new parchment/reference (blue) in comparison with the spectrum of the parchment fragment 113+19 (red).

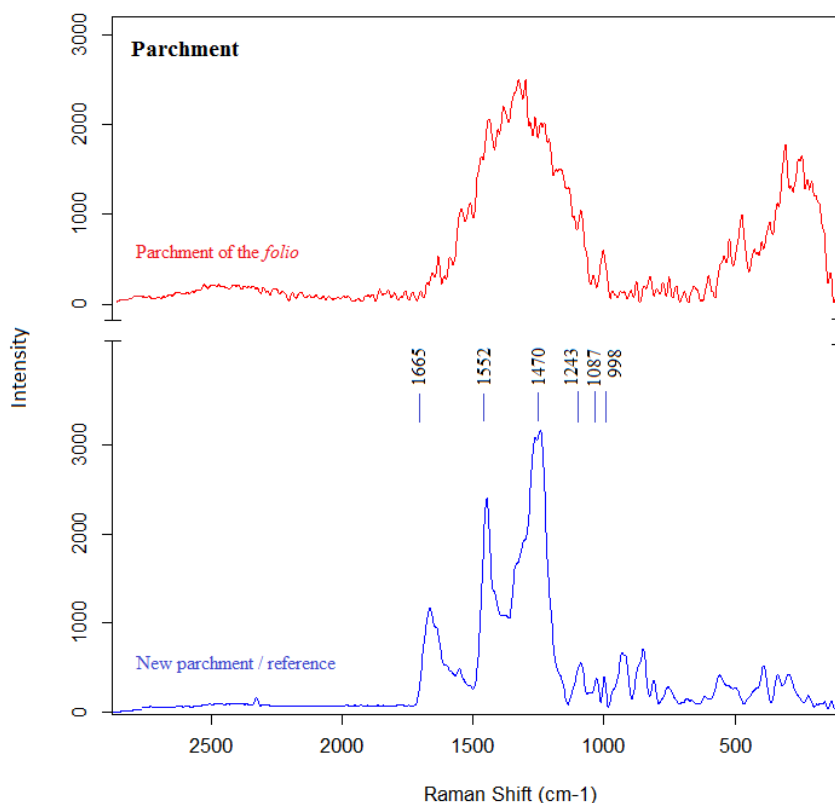


Figure 55. Raman spectrum of the new parchment/reference (blue) in comparison with the parchment spectrum of the *folio* (red).

Bands attributed to the different amino acids constituting the parchment can be seen in the range between 900 and 1000 cm^{-1} , for example at about 1000 cm^{-1} there is a small sharp peak which can be attributed to the ring stretching of phenylalanine [29]. Furthermore, in the parchment spectra a peak at 1087 cm^{-1} attributed to CaCO_3 can be visible. This is due to a possible high content of liming material or calcite applied during the manufacturing of the supporting material [29].

In figure 56 the typical amide I, II and III vibrations are presented [29].

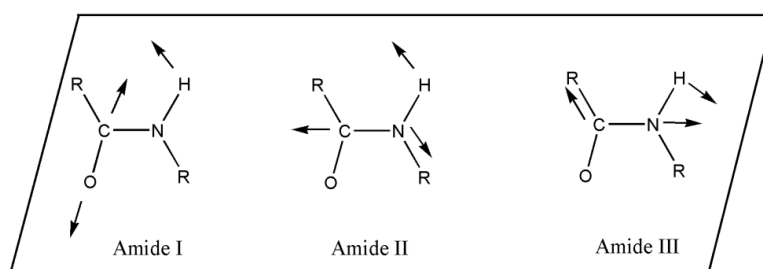


Figure 56. The characteristics amide I, II and III vibrations [29].

Due to the cellulose-based material used for the consolidation treatment, the interpretation of the Raman spectra for the parchment was very difficult. This coating, in fact, covered the peaks, masking the interesting signals. Nevertheless, after several attempts, it was possible to gain results in areas where the cellulose based coating showed a thinner layer.

In all the spectra of the historical Nubian parchments (fragments and *folio*), the peaks are completely broadened. The peak of amide I, especially, is poorly defined and this indicates a degradation, probably due to the hydrolysis of the peptide bonds [29]. Moreover, the phenylalanine ring-stretching band has decreased [30]. It can be assumed that the proteinaceous vellum changed its molecular structure over the centuries.

Investigation on the inks

Fragments

Previous elemental investigations performed with XRF suggested that the main inks possibly applied on the writings are iron gall ink and carbon black for the black/brown ink, red lead and red earth for the red inks. The complementary Raman investigation on the fragments could only confirm the presence of iron gall ink on fragments 113+19, 20 and 5. In figure is presented the comparison between the black ink of fragment 113+19 in comparison with iron gall ink reference.

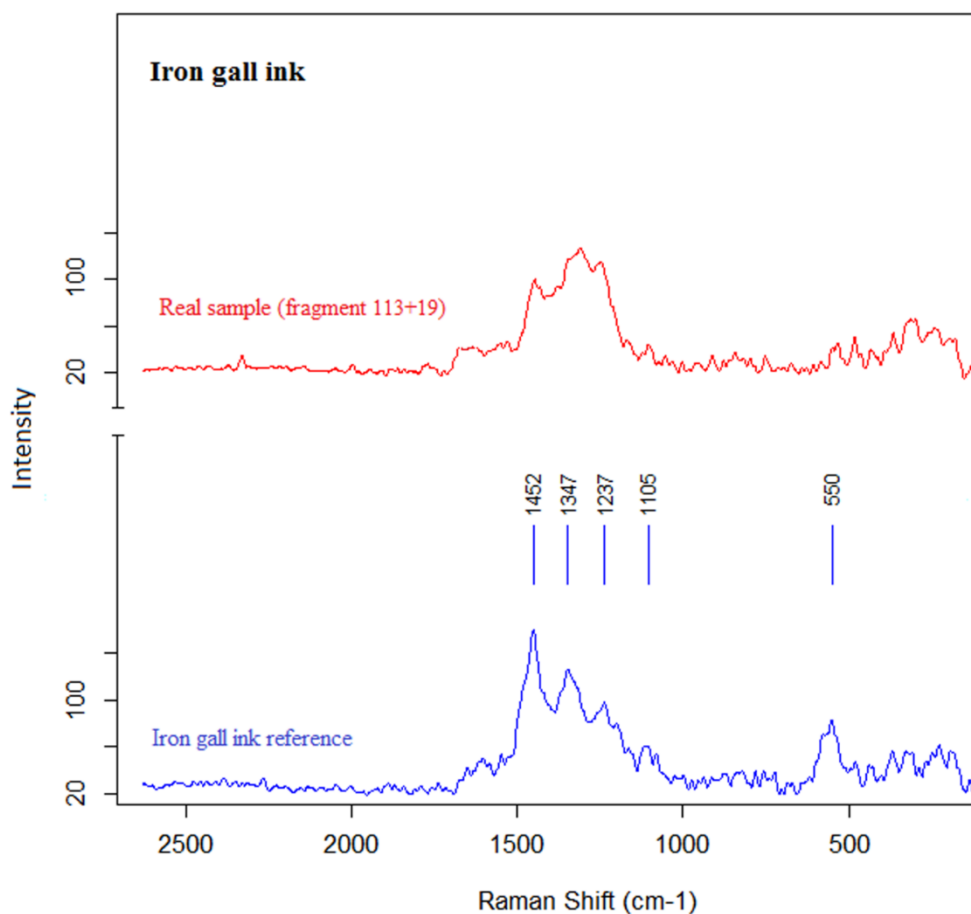


Figure 57. Raman spectrum of the black ink detected on the *rectus* of fragment 113+19 (red) in comparison with iron gall ink reference spectrum (blue).

Tannin based inks have the typical spectral region in the range between 1300-1700 cm^{-1} , in which the aromatic ring vibrations are shown. Two bands around 1200 and 1350 cm^{-1} can be attributed to the C-O stretching vibrations of the ester and the carboxylic groups, respectively. In literature the band at around 1450 cm^{-1} is described to be the most characteristic for iron gall ink [27, 65]. This band might be shifted at higher wavenumbers depending on the tannin species used for the preparation of the ink [27, 65]. An additional broad band at around 550 cm^{-1} can be attributed to the iron complex. Tannins are branched-organic molecules bonded together. Therefore, a large number of vibrations can be visible in the whole spectral range and this can cause some difficulties in the interpretation of the Raman data.

Furthermore, problematic interpretation of the Raman data was also given by the consolidating material applied on the object. Figure 58 shows the broadening of the signals in the area of interest for the detection of iron gall ink (1000 cm^{-1} to 1600 cm^{-1}).

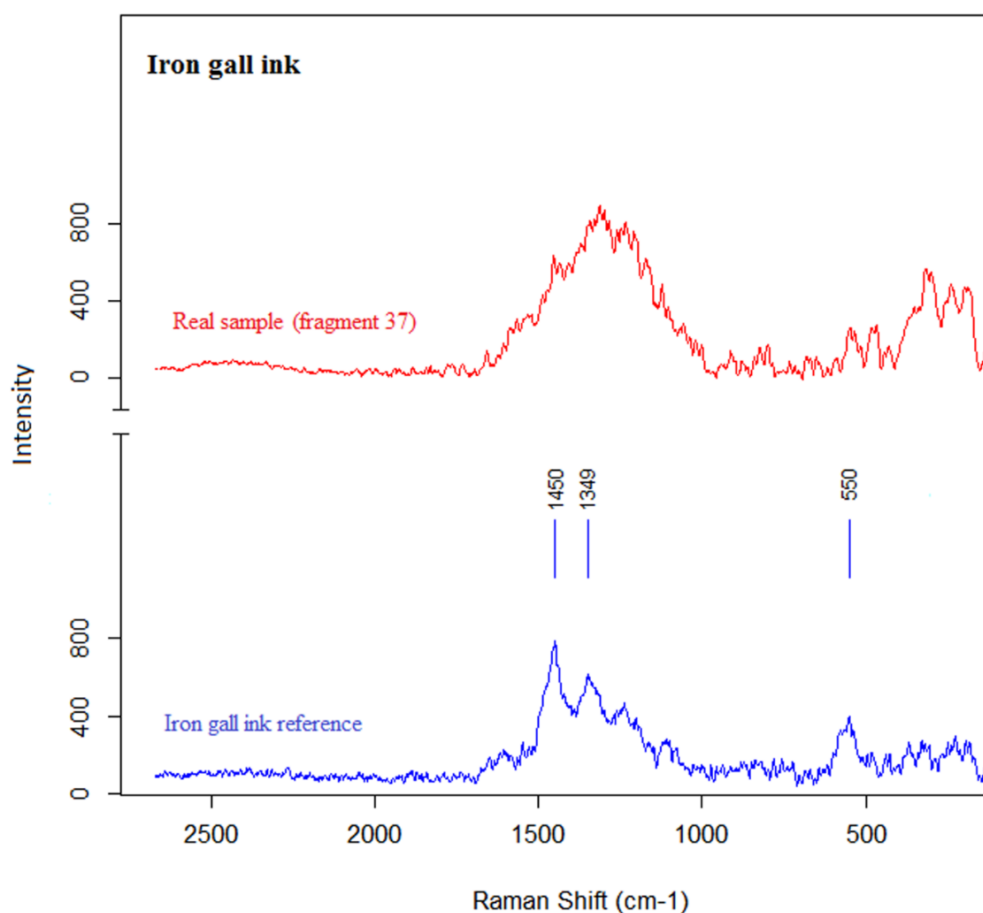


Figure 58. Raman spectrum of the suspected iron gall ink of fragment 20 (red) in comparison with the iron gall ink reference spectrum (blue).

In addition, also the investigations on the red inks were troublesome. Although both red lead and red earth are good Raman scattering materials, no satisfying spectra were obtained. One of the reasons could be attributed to the presence of the cellulose-based consolidation, which partly masked the signals. Moreover, as this consolidating material is subject to thermal degradation, it did not allow the use of higher laser energy, required for a satisfying acquisition of the spectra of these red inks. The combination of these issues leads the measurements to be unsatisfactory. In addition, the typical signals of carbon black ink were covered by the consolidating *patina*, therefore, no identification of the black/brown ink used was possible.

Folio

Raman investigation on the inks applied on the *folio*, were more successful. The results obtained were in accordance with the XRF data previously collected. For the black/brown inks,

carbon black was detected, whereas vermilion was used as red ink. In figure 59 it is possible to compare the acquired spectra of carbon black ink with the reference showing a good match.

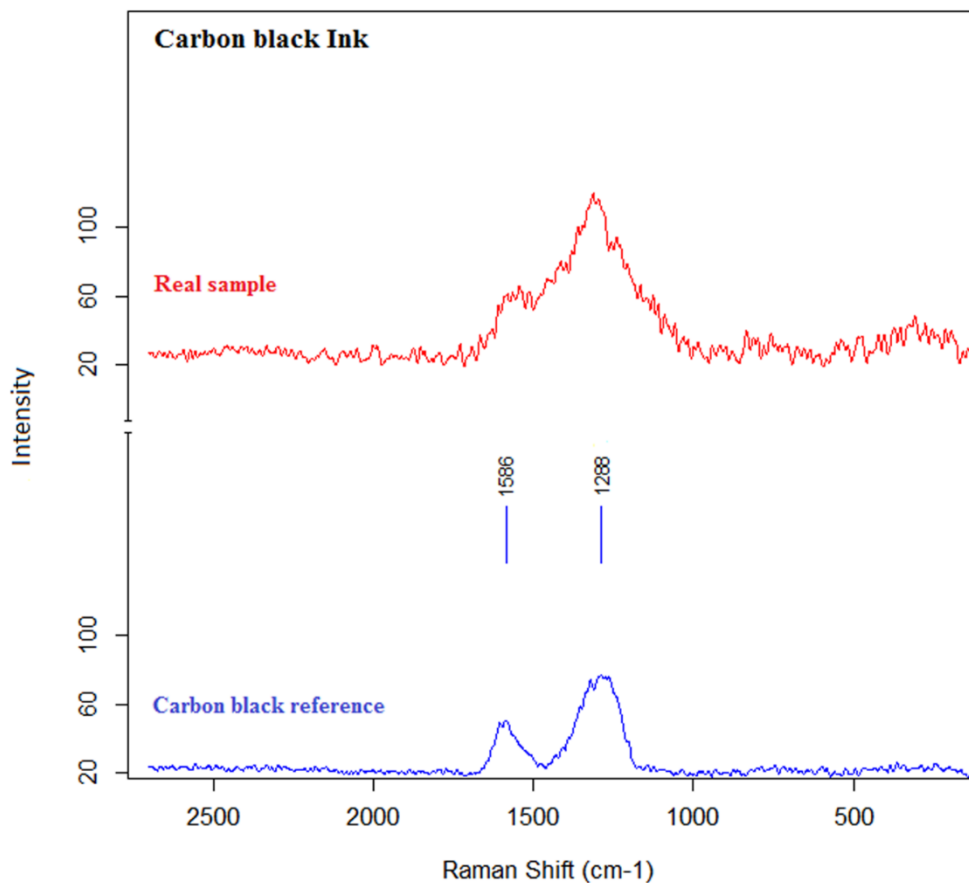


Figure 59. Raman spectrum of carbon black ink of the *folio* (red) in comparison with the carbon black ink reference spectrum (blue).

Amorphous carbon materials show broad bands between 1200 and 1600 cm⁻¹. They can be due to materials of various origins (mineral, vegetal, animal) and different carbon types (coals, chars and soot). Therefore, a difference in shift, width, and relative intensity of the bands can be observed [27, 65].

A perfect match was also achieved for the red ink. The Raman spectrum of cinnabar/vermillion shows only two bands (figure 60): the strong band at 219 cm⁻¹ and a second one less intense at 315 cm⁻¹.

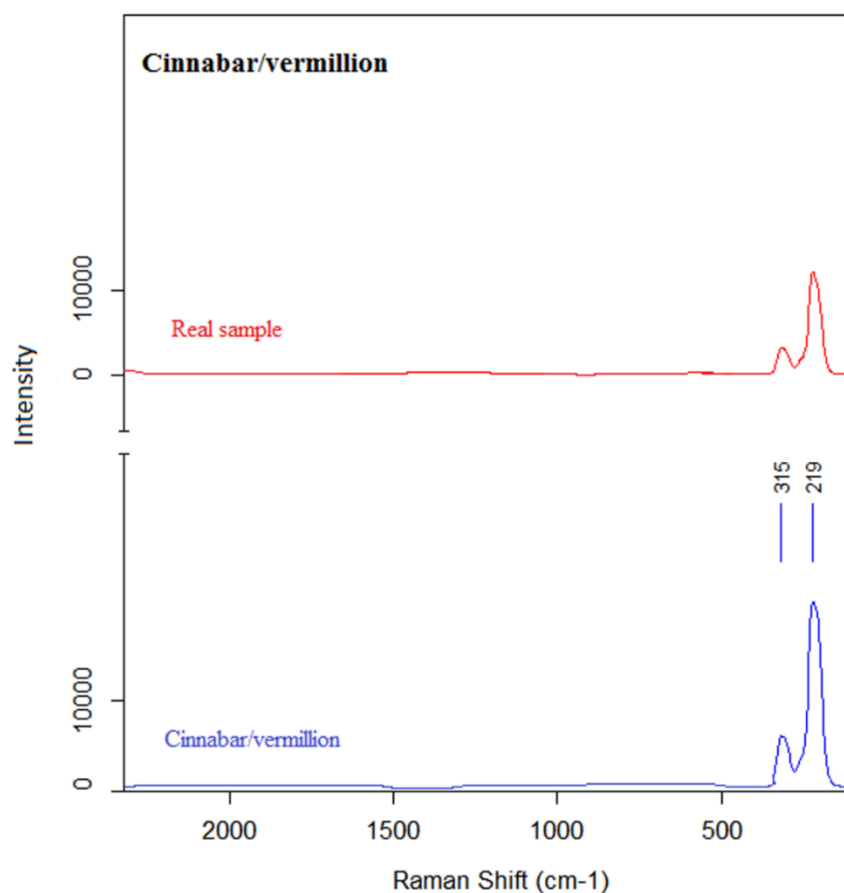


Figure 60. Raman spectrum of red ink detected on the *folio* (red), compared with cinnabar/vermillion reference spectrum (blue).

In summary: Raman spectroscopy confirmed the parchment chemical modification during the centuries, especially evidenced by the broadening of the peak of amide I as well as the decreasing phenylalanine ring stretching. Moreover, due to the presence of the cellulose-based *patina* that covered the main ink peaks, it was only possible to identify and confirm the iron gall ink present in fragments 113+19, 20 and 5 as well as the carbon black and vermillion used in the *folio*.

Chapter 6

Conclusions

For the study of materials and artefacts of cultural value, analytical methods as X-ray fluorescence spectrometry (XRF) and Raman spectroscopy were chosen for their ability to provide information on the chemical nature of the materials and their state of alteration. Furthermore, these techniques can perform non-invasive, fast and multi-elemental analysis. The possibility of using these types of methods is of enormous advantage when sampling is not permitted, as in the case of the objects of this work (fragments and *folio*).

The medieval parchment find from the 11th century, discovered in the today Sudanese Nubia in 2007, represents the most important find of textual material in this region in the last decades. In particular, this work focused on the analysis of six fragments of inscribed parchment and a semi-whole parchment *folio*. As a first conservation-restoration treatment, both, the fragments and the *folio* were treated with a cellulose-based product on both sides.

In particular, X-ray fluorescence offered the first exam of the ancient find providing elemental information. Due to the high penetration depth of the X-ray radiation, the presence of the cellulose-based consolidant layer did not interfere with the analysis of the ancient materials. However, the disadvantage of this technique was that elements of low atomic number such as Na, Mg, Al could not be detected and carbon was not qualitatively determinable. For this reason, carbon-based inks cannot be identified with this method. To overcome such a limitation, Raman

spectroscopy was applied as a complementary technique. The main advantage of this technique was the possibility to distinguish different inks, also of the same colour, by detecting the compound-specific molecular vibrations, characteristic of each chemical structure. For example, it was possible to distinguish between iron gall and carbon black ink, showing that Raman spectroscopy presents the main advantage to investigate both, organic and inorganic compounds. Unfortunately, this technique gave masked results when the cellulose-based consolidants was present in high amount.

For the investigation of the parchment support (fragments and *folio*) both the techniques detected a different composition in comparison with a new freshly prepared parchment as reference material. XRF spot analysis and elemental mapping, in fact detected many elements not present in the reference material. The parchment of the find was richer in elements such as Si, Fe, Ca, K, Cl. The presence of Si and Fe can be attributed to soil and dirt, as the fragments were buried for a long time. Calcium was due to the soaking in lime treatment during the manufacturing steps and the high content of this element in some stains of the *folio* could be ascribed to calcium oxalate from moulds or bacteria to which probably also the presence of K is due. Cl, instead, could be an atmospheric pollutant agent.

Raman spectroscopy confirmed the chemical modification of the Nubian parchments, as in the spectra the peaks were completely broadened compared to the reference parchment spectrum. The peak of amide I (at 1660-1670 cm^{-1}), especially, was poorly defined and this suggests some level of degradation, probably due to the hydrolysis of the peptide bonds of collagen, the main constituent of parchment. Moreover, the prominent phenylalanine ring-stretching band (at about 1000 cm^{-1} in the reference spectrum) has decreased significantly and it can be assumed that the proteinaceous vellum has changed its molecular structure over the centuries. Furthermore, both the techniques confirmed that the chemical composition of parchment could change during time due to atmospheric conditions (such as high temperature and humidity) and biological agents (bacteria and moulds).

XRF analysis on inks (spot analysis and elemental mapping) revealed that the black and the red inks used on the fragments 113+19, 20 and 5 are iron gall ink for the black/brown inks and lead red or a mixture of red lead with red earth for the red writings. For the fragments 70 and 37, the black/brown ink used is a carbon-based ink, as no Fe was detected in the spectra, and the red was identified as a red earth. The black ink of fragment 92, instead, showed no presence of iron and the red ink was recognised as red lead because Pb was found. Moreover, in the *folio* the black

ink was identified as a carbon black ink, whereas the red/orange one is vermillion, due to the presence of Hg and S.

Regarding Raman spectroscopy of the inks, the results of the analysis were very difficult to interpret due to the presence of the cellulose-based *patina*. First, three widely used cellulose-based materials for parchment and paper conservation-restoration were studied (Culminal MC 40, Klucel G and Tylose MH 300) in order to compare their spectra with those obtained for the fragments. Most of the spectra showed the typical peaks of this kind of consolidants, masking the peaks of the pigment. It was only possible to identify and confirm the iron gall ink present in fragments 113+19, 20 and 5 as well as the carbon black and vermillion ink used in the *folio*.

Table 10 summarizes the XRF and the Raman results obtained for the inks. It can be concluded that sometimes Raman spectroscopy did not provide any conclusive information concerning the ink used where the consolidant material has been applied as a rather thick layer.

It is worth noting that based on the XRF and Raman results, fragments 113+19, 20 and 5 could be part of the same manuscript, whereas fragment 92, 70 and 37 could be part of another one. In fact, the first three fragments are characterized by iron gall ink for the black/brown writings and by lead red or lead red/red earth mixture for the red ink, while the analysis of the inks present in the other three fragments revealed carbon black for the black/brown ink.

This difference suggests that the fragments could belong to different manuscripts, probably from different historical periods. The use of carbon black, in fact, is earlier than the use of the iron gall ink.

The red ink recognised in the *folio* was vermillion. The exceptional presence of this pigment suggests that the *folio* could belong to an important ancient manuscript because this red was one of the most precious one used in the antiquity. Probably the manuscript to whom the *folio* belonged was very important from the religious point of view.

The confirmation of all these hypotheses could help archaeologists and philologists about a more precise determination of the geographical and chronological provenance of the Anubis finds.

Within this work, we could strongly support the idea that the identification of inks in a manuscript is useful from historical and curatorial perspective as well as for conservation-restoration purposes. Furthermore, the ability to combine non-invasive techniques as the ones

selected in this work can be used to identify or confirm the ink of a degrading item such as iron gall ink, for treatment purposes or for monitoring to prevent a further deterioration.

Table 10. Summary list of the inks on the fragments and the *folio* analysed by XRF and Raman spectroscopy [66].

Samples	Ink	XRF ^a	Raman ^a	Ink identified
Fragment 113+19	Black	+++	+++	Iron gall
	Red	++	-	Red lead / red lead + red earth
Fragment 20	Black	+++	+++	Iron gall
	Red	++	-	Red lead / red lead + red earth
Fragment 5	Black	+++	+++	Iron gall
	Red	++	-	Red lead / red lead + red earth
Fragment 92	black	-	-	Carbon black
	Red	+++	-	Red lead
Fragment 70	Black	-	-	Carbon black
	Red	+++	-	Red earth
Fragment 37	black	-	-	Carbon black
	Red	+++	-	Red earth
Folio	Black	-	+++	Carbon black
	Red	+++	+++	Cinnabar

^a Conclusive on the identification (+++), supportive (++) or no information provided (-)

List of figures

Figure 1. Electromagnetic spectrum [6].	17
Figure 2. X-ray fluorescence radiation (a) and atomic shells where the electron transitions occur (b) [7].	18
Figure 3. XRF spectrum of a red ink (black spectrum) in comparison with the parchment support (blue spectrum).The typical K- and L-lines of the existing elements can be seen. The red ink is characterised by the presence of Fe and Pb, whereas the elements visible in the parchment are Ca, Si, Cl and K.	19
Figure 4. Scheme of an EDXRF instrument (a) [12] and the X-ray tube (b) [13].	20
Figure 5. Schematic representation of the Silicon Drift Detector (SDD) [14].	21
Figure 6. Portable XRF fluorescence spectrometer instrument, ELIO of XGLab,	22
Figure 7. Scheme of the XRF instrument ELIO used for the elemental mapping.	23
Figure 8. Rayleigh and Raman scattering processes [16].	25
Figure 9. Simplified schematic comparison of Rayleigh and Raman scattering [17].	26
Figure 10. Scheme of the three modes of vibrations for H ₂ O and CO ₂ [16].	27
Figure 11. Schematic diagram of the optical path of the Raman system.	28
Figure 12. Transportable ProRaman-L-Dual-G Raman spectrometer instrument of Enwave Optronics (California, USA).	29
Figure 13. Section of the structure of the skin with the three layers epidermis, derma and hypodermis [35].	33
Figure 14. The hierarchical structure of collagen: from the amino acids chains to the fibres [38].	34

Figure 15. Saponification reaction: triglycerides contained in the animal skin react with $\text{Ca}(\text{OH})_2$ in order to produce free fatty acids.	36
Figure 16. Amino acid cistin is divided into two molecules of cysteine, through the break of disulfide bridge due to the presence of Na_2S	37
Figure 17. Hygroscopic hysteresis of parchment: the process of absorption is different from the process of desorption: the first curve describes how the humidity of parchment increases when the air relative humidity is carried from zero to 100%, whereas the second one shows the opposite behaviour [32].	40
Figure 18. Typical curves of absorption and desorption of parchment: after about 72 hours, the total amount of water becomes constant, and consequently also its weight [32].	41
Figure 19. Particular of a bas-relief found in Corbis dated 2450 BC in which two scribes writing with two <i>calami</i> are sculpted [46].	44
Figure 20. Chemical structure of eumelanin, which it is a complex polymer of 5,6-dihydroxyindole (DHI) and of 5,6-dihydroxyindole-2-carboxylic acid (DHICA) [52].	46
Figure 21. Retene chemical structure. It comes from the burning process of terpenes (saturated hydrocarbons) contained in resinous woods.	47
Figure 22. Chemical structures of gallic acid (a) and tannic acid (pentagalloyc glucose or β -1,2,3,4,6-pentagalloyl-O-D-glucose) (b) [56].	48
Figure 23. Chemical structure of β -1,2,2,3,6-Pentagalloyl-O-D-Glucose (a), where: G = galloyc ester (b), GOG = digalloyc ester, meta-depside bond (c) and GOG = digallyl ester, para-depside bond (d). The molecular weights of all the isomers of PGG are the same (940 g/mol), but the chemical properties depend on the different structure [56].	49
Figure 24. Chemical structure of HHDP (a) formed by the coupling of galloyc groups and converted in elagic acid in aqueous solution (b).	49
Figure 25. Examples of oak gallnuts, fresh (a) and dried (b).	49
Figure 26. Acid-base reaction between gallic acid and Fe^{2+} ions trough which an iron(II) complex is formed [58].	50
Figure 27. Redox reaction in which four molecules of iron sulfate react with four molecules of gallic acid in order to form two molecules of pyrogallate complex and four molecules of water and CO_2 [58].	50
Figure 28. Visualization of new intact and damaged historic parchment at different structural levels [39].	54

Figure 29. Percentage length variation of parchment samples in response to the change of R.H. [32].	55
Figure 30. SEM 50 μm magnifications of glassy surface of parchment after heating treatments [60].	56
Figure 31. Map of the Sudan with the exact place of excavation circled in white.	59
Figure 32. <i>Rectus</i> (a) and <i>versus</i> (b) of the <i>folio</i> (20x24 cm^2).	63
Figure 33. Red under the black ink of the fragment 20 (a) and black and red decorative letter in the <i>folio</i> (b and c), magnification: 16x	64
Figure 34. Red ink on the <i>folio</i> (a) and red ink on fragment 113+19 (b). The second one is more orange than the first one, magnification: 16x	64
Figure 35. Dark spots on parchment, magnification: 16x (a) and 24x (b).	65
Figure 36. Comparison between the yellowish <i>patina</i> on crumbled area (a) and no crumbled area (b) of the <i>folio</i> .	65
Figure 37. Analysed spots (circled in white) of fragment 113+19 <i>rectus</i> (a) and <i>versus</i> (b).	68
Figure 38. Analysed spots (circled in white) of fragment 20 <i>rectus</i> (a) and <i>versus</i> (b).	69
Figure 39. Analysed spots (circled in white) of fragment 5 <i>rectus</i> (a) and <i>versus</i> (b).	70
Figure 40. Analysed spots (circled in white) of fragment 92 <i>rectus</i> (a) and <i>versus</i> (b).	71
Figure 41. Analysed spots (circled in white) of fragment 70 <i>rectus</i> (a) and <i>versus</i> (b).	72
Figure 42. Analysed spots (circled in white) of fragment 37 <i>rectus</i> (a) and <i>versus</i> (b).	73
Figure 43. Analysed spots (circled in white) of the <i>rectus</i> (a) and <i>versus</i> (b) of the <i>folio</i> .	74
Figure 44. Selected area for the mapping of the <i>versus</i> of fragment 70 (a). The imaging and the spectrum show the presence of K (blue), Ca (green) and Fe (red), confirming that the red ink is a earth-based ink and the black ink is a carbon-based ink (b).	75
Figure 45. Mapping image of Ca (a), Fe (b) and K (c) of the <i>versus</i> of fragment 70. Red colour is referred to a high intensity of the elements, whereas the blue shows a low content.	76
Figure 46. Selected area for the mapping of the <i>versus</i> of fragment 70 (a). The mapping and the spectrum show the presence of K (blue), Ca (green) and Fe (red), confirming that the red ink is an earth-based ink (b).	76
Figure 47. Mapping image of Ca (a), Fe (b) and K (c) of the <i>versus</i> of fragment 70. Red colour is referred to a high intensity of the elements, whereas the blue shows a low contents (amount).	77
Figure 48. Selected area for the elemental mapping of the <i>rectus</i> of the <i>folio</i> (a). The images and the spectrum show the presence of Cl (blue), K (green) and Hg (red), confirming that the red ink is vermilion (b).	78

Figure 49. Mapping of Ca (a), Fe (b), K (c) and Hg (d) of the <i>rectus</i> of the <i>folio</i> in figure 48. ...	78
Figure 50. Molecular structure of cellulose monomer.	80
Figure 51. Raman spectra of Culminal MC 40 (green), Klucel G (red) and Tylose MH 300 (blue).	80
Figure 52. Raman spectrum of Culminal MC 40 (blue) in comparison with the parchment spectrum of the <i>folio</i> (red).	81
Figure 53. Raman spectrum of Culminal MC 40 (blue) in comparison with iron gall ink reference spectrum (red).	82
Figure 54. Raman spectrum of the new parchment/reference (blue) in comparison with the parchment spectrum of fragment 113+19 (red).	83
Figure 55. Raman spectrum of the new parchment/reference (blue) in comparison with the parchment spectrum of the <i>folio</i> (red).	84
Figure 56. The characteristics amide I, II and III vibrations [29].	84
Figure 57. Raman spectrum of iron gall ink detected on the <i>rectus</i> of fragment 113+19 (red) in comparison with iron gall ink reference spectrum (blue).	86
Figure 58. Raman spectrum of the suspected iron gall ink of fragment 37 (red) in comparison with the iron gall ink reference spectrum (blue).	87
Figure 59. Raman spectrum of carbon black ink of the <i>folio</i> (red) in comparison with the carbon black ink reference spectrum (blue).	88
Figure 60. Raman spectrum of red ink detected on the <i>folio</i> (red), compared with cinnabar/vermillion reference spectrum (blue).	89

List of tables

Table 1. <i>Rectus</i> and <i>versus</i> of the fragments with their dimensions.	62
Table 2. Comparison between the XRF results of the parchment of the fragments with the reference one.	67
Table 3. XRF results of the analysed spots (circled in white) of the fragment 113+19 <i>rectus</i> and <i>versus</i> . The elements in bold are the main elements, whereas the elements in brackets are of minor content.	68
Table 4. XRF results of the analysed spots (circled in white) of the fragment 20 <i>rectus</i> and <i>versus</i> . The elements in bold are the main elements, whereas the elements in brackets are of minor content.	69
Table 5. XRF results of the analysed spots (circled in white) of the fragment 5 <i>rectus</i> and <i>versus</i> . The elements in bold are the main elements, whereas the elements in brackets are of minor content.	70
Table 6. XRF results of the analysed spots (circled in white) of the fragment 92 <i>rectus</i> and <i>versus</i> . The elements in bold are the main elements, whereas the elements in brackets are of minor content.	71
Table 7. XRF results of the analysed spots (circled in white) of the fragment 70 <i>rectus</i> and <i>versus</i> . The elements in bold are the main elements, whereas the elements in brackets are of minor content.	72
Table 8. XRF results of the analysed spots (circled in white) of the fragment 37 <i>rectus</i> and <i>versus</i> . The elements in bold are the main elements, whereas the elements in brackets are of minor content.	73

Table 9. XRF results of the analysed spots (circled in white) of the *rectus* and *versus* of the *folio*. The elements in bold are the main elements, whereas the elements in brackets are of minor content.

..... 74

Table 10. Summary list of the inks on the fragments and the *folio* analysed by XRF and Raman spectroscopy [66]. 94

Bibliography

- [1] Lahanier C., Amsel G., Heitz C., Menu M., Andersen H. H., Proceedings of the International Workshop on Ion-Beam Analysis in Arts and Archaeology, Nucl. Instrum. Meth. Phys. Res., Pont-A-Mousson, Abbaye des Premontres, France (1986).
- [2] Kriznar A., Munoz M. V., De la Paz F., Respalzida M. A., Vega M., Non-destructive XRF Analysis of Pigments in a 15th Century Panel Painting, 9th International Conference on NDT of Art, Jerusalem, Israel (2008).
- [3] Mantler M., Schreiner M., X-ray Fluorescence Spectrometry in Art and Archaeology, *X-Ray Spectrometry*, 9, 3-17 (2000).
- [4] Leyden D. E., Fundamentals of X-Ray Spectrometry as applied to Energy Dispersive Techniques, Tracor X-ray, Inc., *Mountain View* (1984).
- [5] Glinsman L. D., X-Ray Fluorescence Spectrometry in the Museum Field, Phd Thesis (2004).
- [6] http://www.columbia.edu/~vjd1/electromag_spectrum.htm
- [7] <http://aladdin.utef.cvut.cz/ofat/methods/XRF/index.htm>
- [8] Van Grieken R., Markowicz A., Handbook of X-Ray Spectrometry, Marcel Dekker, Inc. (1993).
- [9] Cesareo R., X-Ray Physics, Nuovo Cimento (2000).
- [10] Chen Z. W., Gibson W. M., Huang H., High Definition X-ray Fluorescence: Principles and Techniques, X-Ray Optics and Instrumentation (2008).

- [11] Gigante G. E., Cesareo R., Non Destructive Analysis of Ancient Metal Alloys by in Situ EDXRF Transportable Equipment, *Radiation Physics and Chemistry*, 4, 689-700 (1998).
- [12] <https://xos.com/technologies/xrf/energy-dispersive-x-ray-fluorescence-ed-xrf/>
- [13] <https://www.orau.org/ptp/collection/xraytubescoolidge/coolidgeinformation.htm>
- [14] <http://www.sgxsensortech.com/content/uploads/2014/10/SDD-300x187.jpg>
- [15] Chalmers J. M., Edwards H. G. M., Hargreaves M. D., *Infrared and Raman Spectroscopy in Forensic Science*, Wiley (2011).
- [16] Smith E, Dent G., *Modern Raman Spectroscopy, a Practical Approach*, Wiley (2005), pp. 2-19.
- [17] <http://www.porous-35.com/appendix-5.html>
- [18] Varella E. A., *Conservation Science for the Cultural Heritage, Applications of Instrumental Analysis*, Springer (2013), pp. 65-80.
- [19] Janssens K., Vittiglio G., Deraedt I., Aerts A., Vekemans B., Vincze L., Wei F., Deryck I., Schalm O., Adams F., Rindby A., Knöchel A., Simionovici A., Snigirev A., Use of Microscopy XRF for Non-destructive Analysis in Art and Archaeometry, *X-Ray spectrometry*, 29, 73-91 (2000).
- [20] Guerra M., Manso M., Pessanha S., Le Gac A., Longelin S., Gíolherme A., Gil M., Seruya A. I., Carvalho M. L., X-Ray Fluorescence Spectrometry as Diagnostic Tool in Characterization and Conservation of Manueline Illuminated Manuscripts, 12th Iberian Meeting on Atomic and Molecular Physics, Sevilla, Spain (2013).
- [21] Burgio L., Clark R. J. H., Hark R., Raman Microscopy and X-Ray Fluorescence Analysis of Pigments on Medieval Renaissance Italian Manuscript Cuttings, *PNAS*, 107, 5726-5731 (2010).
- [22] Hahn O., Malzer W., Kanngiesser B., Beckhoff B., Characterization of Iron-gall Inks in Historical Manuscripts and Music Compositions using X-Ray Fluorescence Spectrometry, *X-Ray Spectrometry*, 33, 234-239 (2004).
- [23] Deneckere A., De Reu M., Martens M. P. J., De Coene K., Vekemans B., Vincze L., De Maeyer P., Vandenabeele P., Moens L., The Use of a Multi-method Approach to Identify the Pigments in the 12th Century Manuscripts Liber Floridus, *Spectrochimica Acta*, 80, 25-132 (2011).

-
- [24] Morsy F. A., El- Sherbiny S. I., Awadalla M., A Systematic Approach to Egyptian Ballpoint Ink Analysis for Forensic Science Application, *Forensic Science*, 4, 1-13 (2005).
- [25] Andermann T., Raman Spectroscopy of Ink on Paper, *Problems of Forensic Sciences*, 46, 335-344 (2001).
- [26] Lee A. S., Mahon P. J., Creagh D. C., Raman Analysis of Iron-gall Inks on Parchment, *Vibrational Spectroscopy*, 41, 170-175 (2006).
- [27] Lee A. S., Otieno-Alego V., Creagh D. C., Identification of Iron-gall Inks with Near-Infrared Raman Mmicrospectroscopy, *Raman Spectroscopy*, 39, 1079-1084 (2008).
- [28] Zieba-Palus J., Kunicki M., Application of the Micro-FTIR Spectroscopy, Raman spectroscopy and XRF method examination of inks, *Forensic Science International*, 40, 164-172 (2006).
- [29] Garp T., Nielsen K, Boghosian S., Study of the Chemical Breakdown of Collagen and Parchment by Raman Spectroscopy, Advanced Study Course (1999).
- [30] Edwards H. G. M., Farwell D. W., Newton E. M., Rull Perez F., Jorge Villar S., Application of FT-Raman Spectroscopy to the Characterization of Parchment and Vellum, I; Novel Information for Paleographic and Historiated Manuscript Studies, *Spectrochimica Acta*, 13, 1223-1234 (2001).
- [31] Gualdoni F., Una Storia del Libro, dalla Pergamena a Ambroise Vollard, Skira (1998), pp.11-12.
- [32] Chimica e Biologia Applicate alla Conservazione degli Archivi, Pubblicazioni degli Archivi di Stato, Ministero per i Beni e le Attività Culturali, Direzione Generale per gli Archivi, 74, 58-105 (2002).
- [33] Nappo L., Pergamene Dipinte e Sistemi di Montaggio. Una Nuova Metodica di Restauro, Campanotto (2008), pp. 17-28.
- [34] Ronald R., the Nature and Making of Parchment, The Elmet Press (1975), p. 13.
- [35] <http://directchemistoutlet.com.au/have-you-moisturised-today/>
- [36] Dolgin B., Bulatov V., Schechter I., Non-destructive Assessment of Parchment Deterioration, *Anal Bioanal Chem*, 17, 1885-1996 (2007).

- [37] Badea E., Poulsen Sommer D. V., Axelsson K., Laresen R., kurysheva A., Miu L., Della Gatta G., Damage Ranking of Historic Parchment: from Microscopic Studies of Fibre Structure to Collagen Denaturation Assessment by Micro DSC, *e-PRESERVATION Science*, 45, 97-109 (2012).
- [38] <http://vearlemedicalart.com/gallery-2/structure-of-tendons/>
- [39] Larsen R., Poulsen D. V., Juchauld F., Jerosh H., Odlyha M., De Groot J., Wang Q., Theodorakopoulos C., Wess T., Hiller J., Kennedy C., Della Gatta G., Badea E., Masic A., Boghosian S., Fessas D., Damage Assessment of Parchment: Complexity and Relations at Different Structural Levels, 14th ICOM-CC Triennial Meeting, The Hague (2005).
- [40] Piez K. A., Truz B. L., Sequence Regularities and Packing of Collagen Molecules, *Mol. Biol.*, 24, 419-430 (1977).
- [41] Della Gatta G., Badea E., Ceccarelli R., Usacheva T., Masic A., Coluccia S., Assessment of Damage on Old Parchments by DSC and SEM, *Thermal Analysis and Calorimetry*, 82, 637-649 (2005).
- [42] Bravo G. A., Trumpke J., 100000 Jahre Leder. Eine Monographie, Basel, Birkhäuser Verlag (1970), p. 112.
- [43] Kennedy J. C., Weiss T. J., Skin Structure; the in Vivo Structure of Collagen, the Structure of Collagen within Parchment, a Review.
- [44] Bicchieri M., Monti M., Piantanida G., Sodo A., Tanasi M. T., Inside the Parchment, 9th International Conference on NDT of Art, Jerusalem, Israel, (2008).
- [45] Hansen E. F., Lee S. N., Sobel H., The Effects of Relative Humidity on Some Physical Properties of Modernum Vellum: Implications for the Optimum Relative Humidity for the Display and Storage of Parchment, *American Institute for Conservation*, 31, 325-342 (1992).
- [46] Giusmano A., Gli Inchiostri nella Storia della Scrittura e della Stampa. Storie, Strumenti, Collezionismi, Editrice Bibliografica (2011), pp. 11-49.
- [47] Jametel M., L' Encre de Chine, son Histoire et sa Fabrication d'après des Documents Chinois, translation of the book of Chen-Ki-Souen, Ernest Leroux (1882), p. 10.
- [48] Guareschi R., Gli Inchiostri da Scrivere, Hoepli (1915), pp. 18-19.
- [49] Fornari U., Fabbricazione di Vernici, Lacche, Inchiostri da Stampa, Hoepli (1913), p. 50.

-
- [50] Cennini C., *Il libro dell'Arte*, edited by Fabio Frezzato, Neri Pozza Editore, (2003) p. 298.
- [51] Bevilacqua N., Borgioli L., Androver Garcia I., *I Pigmenti nell'Arte, dalla Preistoria alla Rivoluzione Industriale*, il Prato (2010), pp. 77-86, 153-164.
- [52] Derby C. D., *Cephalopod Ink: Production, Chemistry, Functions and Applications*, *Mar. Drugs*, 12, 2700-2730, (2014).
- [53] Aceto M., Agostino A., Boccaleri A., Cerutti Garlanda A., *The Vercelli Gospels laid open: an Investigation into the Inks used to write the oldest Gospels in Latin*, *X-Ray spectrometry*, Wiley Inter Science (2008).
- [54] Smith G., *The Chemistry of Historically important Black Inks, Paints and Dyes*, Chemistry Education in New Zealand (2009), pp. 12-15.
- [55] Ruggero D., *Gli Inchiostri Ferrogallici negli Archivi e nelle Biblioteche*, Laboratorio di fisica dell'Istituto per il Restauro e la Conservazione del Patrimonio Archivistico e Librario (2004).
- [56] Haegerman A. E., *Hydrolyzable Tannin Structural Chemistry* (1998).
- [57] Lee A. S., Mahon P. J., Creagh D. C., *Raman Anaysis of Iron gall Inks on Parchment*, *Vibspec*, 2005.
- [58] Neevel J. G., *(Im)possibilities of the Phytate Treatment*, The Iron Gall Ink Meeting, Newcastle (2000), pp. 125-133.
- [59] Hahn O., Rabin I., Wolf T., Kannigieser B., Malzer W., Mantouvalou I., Schade U., Masic A., Weinberg G., *Non-destructive Investigations of the Dead Sea Scrolls*, 9th International Conference on NDT of Art, Jerusalem, Israel, (2008).
- [60] Badea E., Della Gatta G., Usacheva T., *Effects of Temperature and Relative Humidity on Fibrillar Collagen in Parchment: A Micro Differential Scanning Calorimetry (Micro DSC) Study*, *Polymers Degradations and Stability* (2012).
- [61] Krutzsch M., Näser C., Engel P., *Conservation-Restoration of Nubian Leather Finds from the 11th Century*, Paper and Leather Conservation International Conference, Torun (2010).
- [62] Gallo A., *Le Malattie del Libro, le Cure ed i Restauri*, Mondadori (1935), p.79.
- [63] Schenzel K., Fischer S., *Applications of FT-Raman Spectroscopy for the Characterization of Cellulose*, *Lenziger Berichte* (2004), pp. 64-70.

- [64] Szymanska-Chargot M., Cybulska J., Zdunek A., Sensing the Structural Differences in Cellulose from Apple and Bacterial Cell Wall Materials by Raman and FTIR Spectroscopy, *Sensors*, 34, 5543-5560 (2011).
- [65] Bicchieri M., Monti M., Piantanida G., Sodo A., All that is Iron-ink is not always Iron-gall!, *Raman Spectrosc.*, 39, 1074-1078 (2009).
- [66] Apollonia L., Vaudan D., Chatel V., Aceto M., Mirti P., Combined Use of FORS, XRF and Raman Spectroscopy in the Study of Mural Paintings in the Aosta Valley (Italy), *Anal Bioanal Chem*, 23, 2005-2013 (2009).

Acknowledgments

This project was a collaboration between the Institute of Natural Sciences and Technology in Art of the Academy of Fine Arts (Vienna) and the University of Ca' Foscari (Venice).

First of all, I would like to thank my co-advisor Univ.-Prof. Dr. Manfred Schreiner for having given me the opportunity to work in his group and as well the opportunity to expand and improve my knowledge about a really fascinating field of study, the analysis on ancient manuscripts.

I would like to thank my colleagues of the Institute, Rita Wiesinger, Wilfried Vetter, Christine Jiru, Marta Anghelone, Dubravka Jembrih-Simbuerger and Ernst-Georg Hammerschmid for their availability and for providing a nice and stimulant working atmosphere. In particular, I want to thank Bernadette Fruehmann for the help given to me with XRF measurements.

I want to thank my advisor Prof. Dr. Emilio Francesco Orsega and Prof. Dr. Ligia Maria Moretto for always having believed in me. You are not only fantastic professors but also indispensable teachers of life. Thank you for the fantastic days spent together in Vienna.

I also would like to thank my friends Giorgia Zuliani, Fabiola Rocco, Luigi Zanini, Rosa Costantini and Laura Tresin, for the support gave me during my study. Especially, I want to thank my best friend Giulia Babetto, for being my guide in every moment, despite the distance.

Special thanks to Valentina Pintus for being an important friend and an indispensable personal advisor. Thank you for our coffee break rich of chat and useful suggestions.

Particular thanks go to Federica Cappa, a fantastic and peerless friend, without which my stay in Vienna would not have been the same. Thank you for having shared with me good, bad, and crazy moments. You are special!

Last, but definitely not least important, I want to thank my family, my mother, my grandmother my father and Enrico for all the support they gave me. Without them being so loving, I am sure I would not have achieved so much in my life.